# Etude des propriétés spectrales de composés à valence intermédiaire :

# Photoémission et Photoémission Inverse Résonante.

Thèse réalisée dans le groupe du professeur Yves Baer

et

présentée à l'Institut de Physique de l'Université de Neuchâtel pour l'obtention du titre de docteur ès sciences

*Forme réduite de la thèse*

Pascal Weibel

1995

# IMPRIMATUR POUR LA THÈSE

Etude des propriétés spectrales de composés à valence intermédiaire: Photoémission et photoémission inverse résonante

de M. Pascal Weibel

---

UNIVERSITÉ DE NEUCHÂTEL

FACULTÉ DES SCIENCES

La Faculté des sciences de l'Université de Neuchâtel sur le rapport des membres du jury,

Messieurs Y. Baer, M. Grioni, W.-D. Schneider (Lausanne) et D. Malterre (Nancy)

autorise l'impression de la présente thèse.

Neuchâtel, le 21 juin 1995

Le doyen:

H.-H. Nägeli

# Etude des propriétés spectrales de composés à valence intermédiaire: Photoémission et Photoémission Inverse Résonante.

Ce travail est consacré à l'étude de la structure électronique de composés à valence intermédiaire. Dans ces systèmes, les interactions électroniques, à l'origine de comportements complexes sont très fortes. Leur description demande donc des modèles théoriques élaborés.

Dans ce domaine, le cérium est un système paradigmatique. Les fortes corrélations régnant entre les électrons 4f sont à la base de la richesse de la phénoménologie observée. La problématique de l'Ytterbium, également abordée, est similaire.

L'étude de la fonction spectrale obtenue, entre autres, par des techniques de photoémission et de photoémission inverse peut être mis en relation avec la densité d'états électroniques à l'aide d'un support théorique adéquat. Les résultats expérimentaux obtenus grâce à ces techniques sont d'un apport très précieux et font constamment progresser notre compréhension de ces systèmes.

Ce travail est constitué de deux parties distinctes. La première relate les mesures réalisées à l'aide de techniques de photoémission "classiques" UPS (UV Photoemission Spectroscopy) et BIS (Brehmsstrahlung Isochromat Spectroscopy) sur des composés de Cérium et d'Ytterbium [1-4]. La seconde décrit la conception et la mise en oeuvre d'un nouveau spectromètre destiné à l'exploitation de processus résonants en photoémission inverse [5]. Elle contient également les mesures effectuées avec cet instrument sur le cérium [5-7].

La description théorique du comportement des électrons 4f dans ces systèmes s'appuie sur l'Hamiltonien d'Anderson à une impureté. Celui-ci implique l'existence de lois d'échelle en $T_K$ ($T_K$ est la température de Kondo) qui ont en quelque sorte fait office de fil conducteur tout au long de ce travail. Les résultats obtenus s'insèrent de manière convaincante dans ce cadre [1-4]. Cependant, l'accord entre la théorie et l'expérience est loin d'être parfait, en particulier au niveau de la position et de la largeur du pic Kondo [2]. Un effort théorique et expérimental supplémentaire destiné à éclaircir la situation est donc souhaitable.

Les premiers résultats obtenus avec le nouvel instrument sont très concluants [5]. Par rapport aux techniques de photoémission inverse classique, tel que le BIS, les avantages du RIPES (Resonant Inverse Photoemission Spectroscopy) sont de deux ordres. Premièrement, la sélectivité chimique du processus résonant permet d'étudier la fonction spectrale sur le site de cérium et d'identifier clairement les structures découlant de la symétrie 4f [5-7]. L'autre intérêt de cette technique est le confort de mesure obtenu grâce à la forte augmentation de l'intensité (~2 ordres de grandeur). On peut ainsi envisager de mesurer des systèmes délicats (couches minces, échantillons très réactifs,...) où la rapidité de la mesure est primordiale.

Nous avons mesuré de nombreux composés de cérium et obtenus des résultats consistants avec les autres techniques. L'analyse du processus résonant en soit est également riche d'enseignements [7]. Cependant, beaucoup de détails des spectres restent pour l'instant mal comprises. Il est donc aussi nécessaire que souhaitable de poursuivre l'effort théorique si l'on désire accroître notre compréhension dans ce domaine.

EUROPHYSICS LETTERS 1 November 1992

*Europhys. Lett.*, 20 (5), pp. 445-450 (1992)

# Temperature Dependence of the 4*f* Spectral Function in the Kondo System $CeSi_2$: Evidence of the Kondo Resonance Smearing.

D. MALTERRE, M. GRIONI, P. WEIBEL, B. DARDEL and Y. BAER

*Institut de Physique, Université de Neuchâtel - CH-2000 Neuchâtel, Switzerland*

(received 4 May 1992; accepted in final form 1 September 1992)

PACS. 71.28 – Narrow-band systems, heavy-fermion metals: intermediate-valence solids.
PACS. 78.70E – X-ray emission threshold and fluorescence.
PACS. 73.20A – Surface states, band structure, electron density of states.

**Abstract.** – High-resolution photoemission (UPS) and bremsstrahlung isochromat spectra (BIS) have been measured as a function of temperature in $CeSi_2$. In UPS measurements, owing to the high resolution, a weak-temperature evolution can be observed whereas a large effect is shown in BIS. In both cases, the temperature dependence of the spectral function reflects the breakdown of the Kondo state as the low-lying magnetic states become thermally populated. Although the energy resolution of BIS is one order of magnitude larger than the thermodynamic energy scale (the Kondo energy), a significant temperature dependence is observed in BIS spectra.

During the last decade, experimental [1-4] and theoretical [1,5-8] studies in high-energy spectroscopies have greatly contributed to the understanding of the puzzling behaviour of many cerium compounds. It has been shown that the impurity Anderson model provides a unified description of spectroscopic properties such as the 4*f* spectral function and of the single-ion contribution of thermodynamic quantities like the magnetic susceptibility and the specific heat. In this model, the ground state is a singlet resulting from a mixture of different 4*f* configurations. This singlet is separated from a multiplet of excited states by the Kondo energy ($\delta = k_B T_K$) which is a fundamental quantity, since it governs all the physical properties and separates two-temperature ranges. For $T \ll T_K$, the low-energy excitations can be represented by quasi-particles and the system can be considered as a local Fermi liquid as shown in magnetic-susceptibility measurements which reveal a nonmagnetic ground state. On the contrary, for $T \gg T_K$, the description in terms of quasi-particles is no longer valid and the *f* states behave as localized electrons (a local magnetic moment appears on the Ce site). At low temperature, the formation of the singlet ground state is associated with a many-body resonance (the well-known Kondo or Abrikosov-Suhl resonance) just above the Fermi level in the 4*f* spectral function. With increasing temperature well above $T_K$, a smearing of this resonance is expected, reflecting the breakdown of the Fermi-liquid picture. For a long time, photoemission experiments on the valence band have revealed a broad structure near the Fermi level; its intensity, however, was too large to be interpreted as the tail of the Kondo resonance [9]. Moreover, no significant temperature dependence was

observed. More recently, high-resolution photoemission resolved this puzzling behaviour; the main part of the spectral weight is not due to the Kondo resonance but it displays the spin-orbit and the crystal field excitations and it is weakly temperature dependent [10].

Despite these results, it has been recently proposed that the description of the spectroscopic results in terms of the Kondo model is irrelevant; in particular the temperature dependence of the $4f$ spectrum of $CeSi_2$ would be accounted for simply by phonon broadening and the Fermi function [11]. In this alternative approach, it is claimed that there is «no room for an additional temperature effect from the Kondo model». Thereby, the $4f$ spectral function would be insensitive to the breakdown of the Kondo ground state. The aim of this paper is to prove that, on the contrary, the spectroscopic results cannot be interpreted *without* the Kondo model. In particular we show that the temperature dependence of the total $4f$ spectral function, negative- (UPS) and positive-frequency (BIS) parts, cannot be explained by broadening mechanisms and then definitively supports the Kondo model for spectroscopic measurements.

$CeSi_2$ was made by arc-melting the constituent materials several times under argon atmosphere and it was characterized by X-ray powder diffraction patterns. It crystallizes in the tetragonal $\alpha$-$ThSi_2$ structure. Magnetic measurements at low temperature reveal the Pauli-paramagnet behaviour expected for the stoichiometric compound. The different spectroscopic measurements were performed in an apparatus combining UPS, XPS and BIS. The sample could be cooled with a closed-cycle He refrigerator to about 15 K. In UPS the overall energy resolution, estimated from the width of the Fermi step, is better than 20 meV. BIS spectra were obtained with a photon energy of 1486.6 eV and a total energy resolution of 0.6 eV was achieved. The pressure was in the low $10^{-10}$ Torr range during the measurements. The sample was cleaned by repeated scraping with a diamond file until no oxygen contamination (O $1s$ and O $2p$ photoemission signals) could be detected.

High-resolution photoemission spectra of $CeSi_2$ have previously been measured and interpreted in the framework of the Anderson model by Patthey *et al.* [12]. Thus, we only briefly present the photoemission results and focus on the BIS spectra. The photoemission spectra reflect two kinds of final states: final states with a $4f^0$ character which yield a broad feature near $E = -2$ eV and final states with mainly a $4f^1$ character which contribute to the spectral weight near the Fermi level $E_F$. In fig. 1, the $4f$ photoemission spectra near $E_F$ are reported at $T = 15$ K and $T = 300$ K; the spectral weight just below $E_F$ is slightly larger than in the previous measurements of Patthey *et al.* [12]. This difference suggests that the present sample is closer to the exact stoichiometry, since the electronic configuration is very sensitive to the vacancies in this system and the Kondo temperature rapidly decreases with increasing $y$ in the $CeSi_{2-y}$ alloys [13-15]. The $T = 15$ K and $T = 300$ K spectral functions for the Anderson Hamiltonian have been calculated in the noncrossing approximation (NCA) and qualitatively reproduce the experimental measurements with the following parameters: $\varepsilon_f = -1.5$ eV, hybridization strength $\Delta = 88$ meV, spin-orbit separation $\Delta_{SO} = 300$ meV. The fundamental crystal field level is a doublet separated from excited quartet states by 35 meV. The calculated spectra are convoluted with a Gaussian (20 meV FWHM) to simulate the instrumental resolution. With these parameters, we obtain $n_f = 0.96$ for the $4f$ occupation number and $T_K = 50$ K for the Kondo temperature; these values are close to the estimations of Patthey *et al.* ($n_f = 0.97$ and $T_K = 35$ K). The two observed structures just below $E_F$ and at $E = -280$ meV represent the crystal field and spin-orbit excitations, respectively. In contrast to earlier poor-energy-resolution experiments, these features are not interpreted as accounting exclusively for the Kondo resonance which only contributes to the spectral weight in the Kondo energy-range ($k_B T_K \approx 5$ meV) below $E_F$. The Kondo model gives a physical interpretation of the different features of the photoemission spectral function, and it correctly predicts the observed temperature dependence of the spectral *shape* and the

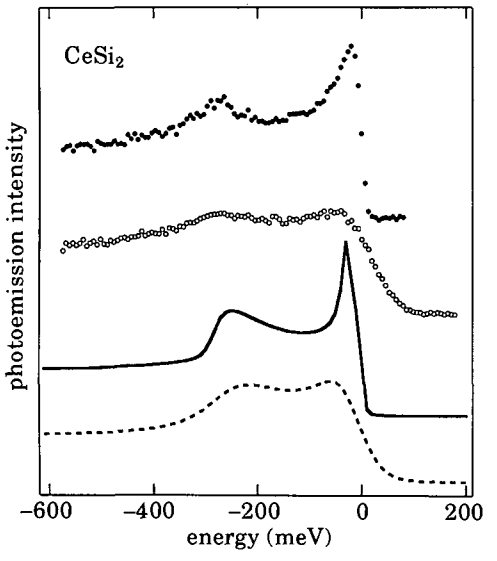


Fig. 1.

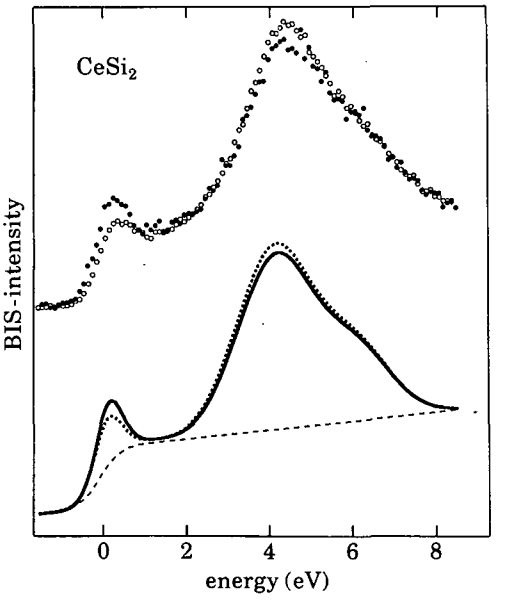


Fig. 2.

Fig. 1. – Experimental 4*f* photoemission spectral functions obtained as in ref. [14] from the difference between HeI and HeII spectra at $T = 15$ K (full circles) and $T = 300$ K (open circles). Solid and dashed lines represent the calculated spectra at the same temperatures: $T = 15$ K, --- $T = 300$ K.

Fig. 2. – Experimental BIS spectra for two temperatures $T = 15$ K (full circles) and $T = 300$ K (open circles) and calculated 4*f* spectral functions for $T = 15$ K (full line) and $T = 300$ K (dotted line). The peaks near $E_F$ were convoluted by a Gaussian (0.6 eV FWHM) to account for the experimental resolution, and the high-energy structures ($4f^2$ final states) were split in two lines and broadened by a Gaussian (2 eV FWHM) to account for the multiplet effect.

invariance of the spectral *integrated weight*. The empirical model of ref. [11] could also produce similar spectra, but only with arbitrary defined final states, and by invoking questionable broadening mechanisms [16]. Moreover, that approach is incompatible with the experimental BIS results discussed below.

Figure 2 shows the inverse photoemission spectrum of $CeSi_2$ for $T = 15$ K and $T = 300$ K. A significant temperature dependence is clearly observed: the intensity of the low-energy structure is depleted with increasing temperature. This temperature dependence is reproducible and cannot be due to oxidation effects (the cleanliness of the sample was regularly checked during these BIS measurements). The two structures at $E = 0.5$ eV and $E = 5$ eV represent final states with a $f^1$ and $f^2$ character, respectively, since the initial state is a mixture of $4f^0$ and $4f^1$ configurations. As demonstrated by calculations in the framework of the Anderson model [8], the $f^1$ structure contains two contributions if crystal field interactions are neglected: the Kondo resonance at $\delta = k_B T_K$ and a spin orbit satellite at $\delta + \Delta_{SO}$ ($\Delta_{SO} \approx 300$ meV in cerium), but owing to the poor energy resolution of BIS ($\Delta E = 0.6$ eV), only one peak about 0.8 eV wide is observed. The two contributions are both depleted with the characteristic Kondo temperature scale [8]. This temperature dependence can be qualitatively understood [17]: the singlet ground state is a hybridized state ($n_f < 1$) separated by the Kondo energy ($k_B T_K$) from the excited magnetic states ($n_f = 1$). At low temperature ($T \ll T_K$), only the singlet ground state is populated and the low-energy BIS structure reflects the amplitude of the $4f^0$ configuration in the initial state. With increasing

temperature, the excited states are progressively populated ($\langle n_f \rangle$ increases) leading to a reduction of the $f^0$ amplitude in the initial state. As a consequence, the weight of the BIS $f^1$ structure decreases, following the evolution of $\langle 1 - n_f \rangle$ with temperature, and a transfer of spectral weight from the low-energy peak to the high-energy structure is actually expected. For a quantitative analysis, we have simulated the spectral function for finite temperatures with a simplified approach. As shown in NCA calculations, the temperature dependence of the $4f$ occupation number exhibits a scaling law in $T/T_K$ (ref. [8]; fig. 13 and 14). With the hybridization strength used for $CeSi_2$, the thermal average $\langle n_f \rangle$ increases from 0.965 at $T = 15$ K to 0.977 at 300 K. By assuming that, at a finite temperature $T$, $\langle n_f \rangle$ results from a statistical admixture of the ground state with $n_f = 0.96$ and excited states with $n_f = 1$, we deduce the respective weight, $a(T)$ and $b(T)$, of these two different states. The finite-temperature spectra are simply calculated from a combination of the BIS spectra corresponding to the ground and excited states weighed by their respective population in the initial state:

$$A(\omega, T) = a(T) A_{GS}(\omega) + b(T) A_{ex}(\omega), \tag{1}$$

$A_{GS}(\omega)$ is the $T = 0$ K spectrum calculated in the Gunnarsson-Schönhammer model [5] with the following parameters: $U_{ff} = 5.7$ eV, $\varepsilon_f = -1.5$ eV, $\Delta_{SO} = 300$ meV and $\Gamma = 65$ meV. $A_{ex}(\omega)$ is the calculated spectrum for the excited magnetic states. As these excited states have a $4f^1$ character, they only contribute to the $f^2$ structure in the BIS spectrum. In order to compare with experimental spectra, the calculated spectra are convoluted with a Gaussian (0.6 eV FWHM) to account for the energy resolution. As the shape of the $4f^2$ structure is dominated by multiplet effects, an additional broadening of this feature is also made. Finally, we add a simple analytical function which simulates the contributions of the non-$f$ states and of the inelastic background (dashed curve in fig. 2). This background is somewhat arbitrary and a different choice could only slightly modify the quantitative analysis. The resulting spectra for $T = 15$ K and $T = 300$ K (solid and dashed lines in fig. 2) are in satisfactory agreement with the experimental results. It is clear that the two mechanisms proposed in ref. [11] to account for the photoemission spectral function (phonon broadening and Fermi function) cannot explain this important effect. Both mechanisms only affect the shape of the spectra on a moderate energy range (about 100 meV at room temperature) but do not modify the integrated spectral weight. Since a transfer of intensity from the vicinity of the Fermi energy to $E = 5$ eV is unambiguously observed, the BIS measurements definitively exclude an interpretation in terms of these simple mechanisms and demonstrate the validity of the Kondo model.

A contrasted temperature dependence is observed in UPS and BIS. Only the shape of the UPS spectrum within 0.2 eV below $E_F$ is modified with increasing temperature whereas a transfer of intensity over a few eV is shown in BIS. This difference results from the particular couplings of the excited final states to the initial state in the two techniques. In fact, in the $N + 1$ and $N - 1$ energy diagrams, there are two kinds of final states in the low-energy range corresponding to the $4f^1$ structure: hybridized $4f^1$-$4f^0$ states like the ground state and nonhybridized $4f^1$ states. In photoemission, the ground state is only coupled to the hybridized states, since the removal of an $f$ electron yields final states with a $4f^0$ contribution. The thermally populated first excited states have a $4f^1$ character and are also coupled to the hybridized final states. Thus, only a tiny temperature dependence originating from the variation of $\langle n_f \rangle$ is expected in photoemission. In BIS, the addition of one $4f$ electron modifies the selection rules. Due to its $4f^0$ part, the ground state is coupled to the hybridized as well as to the nonhybridized final states (fig. 3). Nevertheless, in contrast to photoemission, the thermally excited states do not contribute to the $4f^1$ structure, since only the transitions toward $4f^2$ final states are allowed.

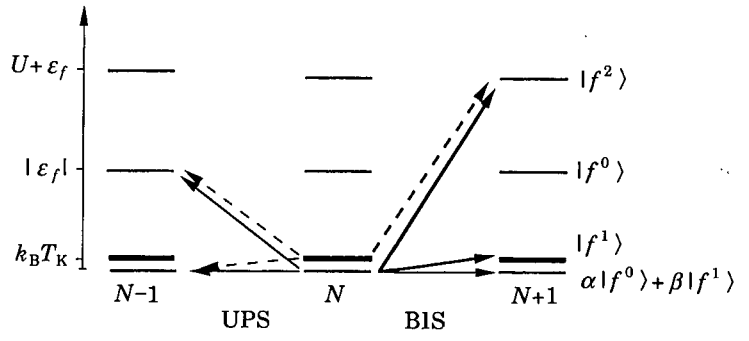


Fig. 3. – Schematic energy diagrams (discrete levels corresponding to the zero bandwidth limit) for the initial ($N$) and final states of photoemission ($N-1$) and inverse photoemission ($N+1$). The thin horizontal lines represent hybridized $f^1$-$f^0$ levels, whereas the thick lines represent multiplets of excited magnetic states ($f^1$). For UPS and BIS, the solid and dashed arrows illustrate, respectively, transitions from the ground state and the excited states which become thermally populated when $T > T_K$. The population of the excited magnetic states induces a transfer of spectral weight from the low energy to the high intensity in BIS because these excited states are not coupled to the final ($4f^1$) states, whereas in photoemission no significant modification is expected. For clarity, we have omitted the crystal field and spin-orbit excitations but the generalization is straightforward and it leads to the appearance of satellites in the UPS and BIS spectra.

As a consequence, a strong spectral weight transfer from the $4f^1$ structure to the $4f^2$ structure reflecting the variation of $\langle 1 - n_f \rangle$ is predicted.

To summarize, we demonstrate in this study that the temperature dependence of the 4*f* spectral function of $CeSi_2$ is well described in the framework of the Anderson model. Although its negative-frequency part (photoemission spectrum) only exhibits a very weak temperature effect, the positive-frequency part (BIS spectrum) shows that, with increasing temperature, there is a transfer of spectral intensity from the $4f^1$ to the $4f^2$ structure. This effect reflects the smearing of the Kondo resonance and the breakdown of the Kondo ground state. At zero temperature, the singlet ground state can be considered to be a Fermi liquid and the spectral function reveals the quasi-particle weight at the Fermi level. On the contrary, when $T \gg T_K$, the heavy quasi-particles disappear, the spectral function near $E_F$ vanishes reflecting the breakdown of the Fermi-liquid picture and the formation of a localized moment. This result shows that, despite its poor energy resolution, BIS is sensitive to the low-energy excitations which govern the physical properties of correlated materials.

* * *

We are grateful to J. HUBSCH (service commun de magnétisme de l'Université de Nancy I) for his magnetic measurements. Two of us (DM and MG) would like to thank D. LIBAN, A. BURKHARDT and D. RASKOLNIKOV for their constant encouragements and support. This work has been supported by the Fonds National Suisse de la Recherche Scientifique.

## REFERENCES

[1] GSCHNEIDNER jr. K. A., EYRING L. and HÜFNER S. (Editors), *Handbook on the Physics and Chemistry of Rare-Earths*, Vol. 10 (Elsevier Science Publisher B.V.) 1987, p. 103.

[2] HILLEBRECHT F. U., FUGGLE J. C., SAWATZKY G. A., CAMPAGNA M., GUNNARSSON O. and SCHÖNHAMMER K., *Phys. Rev. B*, 30 (1984) 1777.

[3] FUGGLE J. C., HILLEBRECHT F. U., ZOLNIEREK Z., LÄSSER R., FREIBURG CH., GUNNARSSON O. and SCHÖNHAMMER K., *Phys. Rev. B*, 27 (1983) 7330.
[4] ALLEN J. W., OH S. J., GUNNARSSON O., SCHÖNHAMMER K., MAPLE M. B., TORIKACHVILI M. S. and LINDAU I., *Adv. Phys.*, 35 (1986) 275.
[5] GUNNARSSON O. and SCHÖNHAMMER K., *Phys. Rev. B*, 28 (1983) 4315.
[6] KOJIMA H., KURAMOTO Y. and TACHIKI M., *Z. Phys. B*, 54 (1984) 293.
[7] GREWE N., *Z. Phys. B*, 53 (1983) 271.
[8] BICKERS N. E., COX D. L. and WILKINS J. W., *Phys. Rev. Lett.*, 54 (1985) 230; *Phys. Rev. B*, 36 (1987) 2036.
[9] LYNCH D. W. and WEAVER J. H., in *Handbook on the Physics and Chemistry of Rare-Earths*, edited by K. A. GSCHNEIDNER jr., L. EYRING and S. HÜFNER, Vol. 10 (Elsevier Science Publisher B.V.) 1987, p. 231.
[10] PATTHEY F., IMER J. M., SCHNEIDER W.-D., BECK H., BAER Y. and DELLEY B., *Phys. Rev. B*, 42 (1990) 8864.
[11] JOYCE J., ARKO A. J., LAWRENCE J., CANFIELD P. C., FISK Z., BARTLETT R. J. and THOMPSON J. D., *Phys. Rev. Lett.*, 68 (1992) 236.
[12] PATTHEY F., SCHNEIDER W.-D., BAER Y. and DELLEY B., *Phys. Rev. Lett.*, 58 (1987) 2810.
[13] YASHIMA H., MORI H., SATOH T. and KOHN K., *Solid State Commun.*, 43 (1982) 193.
[14] LEE W. H., SHELTON R. N., DHAR S. K. and GSCHNEIDNER jr. K. A., *Phys. Rev. B*, 35 (1987) 8523.
[15] SHAHEEN S. A. and SCHILLING J. S., *Phys. Rev. B*, 35 (1987) 6880.
[16] PATTHEY F., SCHNEIDER W.-D., GRIONI M., MALTERRE D., BAER Y. and DELLEY B., comment submitted to *Phys. Rev. Lett.*
[17] MALTERRE D., GRIONI M., WEIBEL P., DARDEL B. and BAER Y., *Phys. Rev. Lett.*, 68 (1992) 2656.

Z. Phys. B 91, 337–341 (1993)

ZEITSCHRIFT
FÜR PHYSIK B


# Temperature dependence of the Kondo peak in photoemission spectra of $YbAgCu_4$

**P. Weibel[1], M. Grioni[1], D. Malterre[1], B. Dardel[1], Y. Baer[1], M.J. Besnus[2]**

[1] Institut de Physique, Université de Neuchâtel, CH-2000 Neuchâtel, Switzerland
[2] IPCMS/GEMM, Institut de Physique, F-67084 Strasbourg, France

Reeeived: 3 January 1993 / Revised version: 29 January 1993

**Abstract.** Temperature dependent photoelectron spectra of the heavy fermion $YbAgCu_4$ show that the Kondo resonance is strongly depressed with increasing temperature. The observed reduction is fully consistent with the predictions of the Anderson impurity model, and reveals the transition from a Fermi liquid at low temperature to localized moments above the characteristic Kondo temperature. Despite this important experimental confirmation of the model, discrepancies exist between the experimental and calculated linewidth of the resonance. It is argued that a more realistic treatment of the photoemission process would improve the agreement between theory and experiment.

## I. Introduction

The degenerate Anderson impurity model provides a well-established conceptual framework for the description of a class of lanthanide and actinide materials that exhibit the peculiar Kondo phenomenology (non-magnetic ground state, non-integer valence, low-temperature anomalies of the static and dynamic electronic properties) [1,2]. An important achievement of the model is the unified treatment of thermodynamic properties and high energy spectroscopic results. Important contributions to a better understanding of the model have indeed come over the years from the analysis of its spectral properties. Calculational schemes devised for the simplest case of cerium [3, 4] have been consistently used to interpret experimental core level and valence photoemission (PES) and inverse photoemission (BIS) data [4–7]. The qualitative, and in some cases even quantitative [8], agreement between the parameters obtained from the analysis of the spectroscopic data and the parameters derived from measurements of low-energy properties like the specific heat or the dynamic susceptibility, has been generally regarded as an important indication of the internal consistency and soundness of the description of these materials within the Anderson model.

A unique feature of the Kondo model is the appearance, just above $E_F$ for cerium, of a sharp many-body resonance in the $4f$ spectral function. Its position and width reflect the characteristic energy scale ($k_B T_K$) of the spin fluctuations that dominate the low temperature properties of these materials. The intensity of the Kondo resonance exhibits a strong temperature dependence that reflects the thermal depopulation, with increasing temperature, of the singlet ground state of the Anderson hamiltonian, and the population of excited (unhybridized) states. The existence of a Kondo scale for the temperature dependence of the integrated spectral intensity near $E_F$ is therefore a strong and characteristic prediction of the Kondo model, susceptible of experimental verification.

Although the first hints that this scenario might actually be experimentally verified came from high resolution PES measurements [9], the temperature dependence of the photoemission spectra of Ce compounds is very small [4]. On the contrary the electron addition spectrum observed with BIS is expected to exhibit a strong temperature dependence, as a consequence of the location above $E_F$ of the Kondo resonance and of the symmetry of the final states. Recent BIS results on $CePd_3$ ($T_K \sim 240$ K) [10] and $CeSi_2$ ($T_K \sim 50$ K) [11] have provided a definitive experimental confirmation of this theoretical prediction.

Due to the electron-hole symmetry of the Anderson Hamiltonian the strong temperature dependence of the BIS spectra of Ce ($n_f \sim 1$) compounds must be observed in the PES spectra of Yb ($14\text{-}n_f \sim 1$) compounds. No qualitatively new phenomenology can be expected, since the PES spectrum of an Yb impurity coincides with the BIS spectrum of a Ce impurity after trivial renormalization of the parameters. Nevertheless a PES study of Yb materials is very appealing because it offers the possibility to observe the main part of the Kondo resonance (as opposed to its tail, visible in PES spectra of Ce) with a

resolution which is one to two orders of magnitude better than the present experimental resolution of BIS.

Recent reports of temperature dependent PES investigations of mixed-valent Yb compounds by two different groups have yielded apparently irreconciliable results. While one group [12] observes a clear temperature dependence of the $4f$ spectral weight, a temperature invariant $4f$ spectral function is claimed for the same materials by the other group [13]. This discrepancy concerns a crucial point and urgently calls for an independent examination because the temperature dependence of the Kondo peak is a necessary consequence of the Anderson model. Failure to observe it would question at a very fundamental level the validity of the interpretation of spectroscopic properties within the Kondo picture. We have therefore investigated with high resolution PES the temperature dependence of the $4f$ spectral function of $YbAgCu_4$, a material that exhibits a clear Kondo behavior. In this paper we show that the results of this investigation are perfectly compatible with the temperature dependence predicted by the model, although at present unexplained discrepancies exist between predicted and experimentally observed lineshapes.

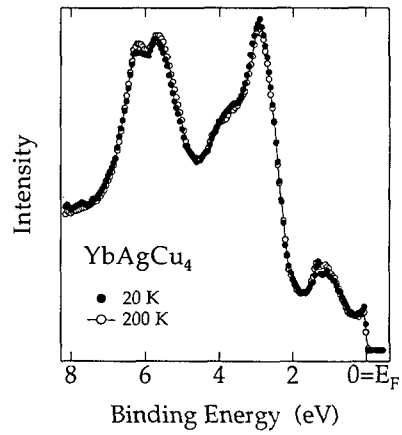


**Fig. 1.** Valence band spectra of $YbAgCu_4$ at 20 K and 200 K, collected with medium resolution at 40.8 eV photon energy. The spectra have been normalized to the peak intensity of the Cu $3d$ band at 3 eV. The Yb surface and bulk signal corresponding to final states with $4f^{13}$ character is observed between 2 eV and the Fermi level

## II. Results and discussion

$YbAgCu_4$ exhibits properties typical of a dense Kondo or heavy fermion system. The magnetic susceptibility that follows a Curie-Weiss behavior in the range 100 K–300 K has a maximum near 30–35 K [14–16], and no evidence exists of magnetic order down to 0.05 K. The $4f$ contribution to the specific heat similarly presents an anomaly at 33.5 K and a moderately high $\gamma(0)$ value of 245 $mJ/K^2$ mol. These data as well as neutron scattering [17] and NMR [18] results indicate a Kondo behavior with a Kondo temperature $T_K \sim 150$ K and a fully degenerate ($N=8$) $J=7/2$ ground state. Further analysis has however shown that the existing data can also be interpreted in terms of a Kondo temperature $T_K \sim 60$ K and a level scheme similar to that of isoelectronic $YbAuCu_4$, resulting from a cubic crystal field with an overall splitting of 80 K [19].

The $YbAgCu_4$ polycristalline sample was prepared in an argon arc furnace. The sample was mounted on the tip of a closed-cycle He refrigerator, and its temperature could be varied between 20 K and 300 K. Clean surfaces were prepared by fracturing or scraping the sample with a diamond file in a vacuum of $1 \times 10^{-10}$ torr. The light source was a He resonance lamp (photon energies 21.2 eV (He I) and 40.8 eV (He II)). Photoelectron spectra were collected by a spherical analyzer with a total energy resolution of 20–25 meV.

Figure 1 shows valence band PES spectra of $YbAgCu_4$ at 20 K and 200 K. The prominent double feature centered at 3 and 6 eV are the Cu $3d$ and Ag $4d$ derived bands. The Yb $4f$ signal is located between $E_F$ and 2.5 eV (corresponding to $4f^{13}$ final states) and below $\sim 5$ eV ($4f^{12}$ final states) [20], but, due to the presence of the Cu $3d$ and Ag $4d$ bands, it is only possible to identify Yb $4f$ features in the region between 2 eV and the Fermi level. The Yb $4f$ signal reflects here two distinct and partially overlapping contributions. The first is bulk emission from hybridized initial states with mixed $f^{13}$ and $f^{14}$ character: this contribution consists of a sharp peak close to the Fermi level and of a spin orbit replica at 1.4 eV. The second contribution is from divalent ($f^{14}$) Yb ions at or near the sample surface and consists of a broader (0.5–1 eV) peak centered at $\sim 1$ eV and of a spin orbit replica which is masked by the Cu $3d$ band. The spectra of Fig. 1 have been normalized to the peak intensity of the Cu $3d$ band. It is important to stress that when spectra collected at different temperatures are normalized in this natural way, they also overlap within the statistical noise in correspondence of all other non-$f$ features, and namely in the energy range 0.2–0.5 eV, immediately below the sharp $4f$ peak near $E_F$. This guarantees that possible changes in the large surface peak do not affect the determination of the temperature dependence of the bulk $4f$ feature. The high resolution spectra presented below have been accordingly normalized at 0.4 eV.

The temperature dependence of the $4f$ spectral function has been carefully measured on a surface, prepared by fracturing the sample, that presented the largest ratio of bulk to surface signal. The raw spectra collected with high energy resolution at selected temperatures between 20 K and 260 K are shown in Fig. 2. The 20 K spectrum presents a sharp feature close to $E_F$. A comparison with spectra taken at 21.2 eV photon energy (not shown), with strongly reduced $4f$ cross section, confirms the $4f$ character of this feature, which is superposed on a flat background from states of different symmetry. At each temperature we have modelled the contribution of band states to the total spectrum by a step-like function obtained by multiplying a constant and temperature independent density of states by the appropriate Fermi function. In Fig. 2, for clarity, only the contribution corresponding to $T=260$ K is shown. The maximum of the $4f$ structure

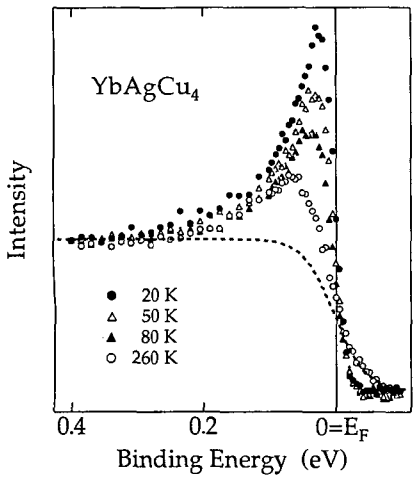


**Fig. 2.** High resolution spectra showing the temperature evolution of the Kondo peak. The dashed line represents the contribution from a flat density of band states at $T=260$ K. The reduction of the peak intensity cannot be simply explained by the temperature dependence of the Fermi function

occurs at 25 meV. The width at half maximum of the asymmetric tail is 75 meV, and the breadth of the peak's leading edge ($\sim$40 meV) is larger than the Fermi cutoff for $T=20$ K, broadened by the experimental resolution ($<25$ meV). The intensity of the $4f$ peak is strongly depressed with increasing temperature, and its maximum progressively shifts to higher binding energy. Because of the imposed temperature invariance of the Cu $3d$ peak, the evolution of the spectra of Fig. 2 reflects a real temperature dependence of the $4f$ spectral function and not an artifact due to an incorrect normalization. A similar temperature dependence has been observed on surfaces prepared by scraping, either at $RT$ or at 20 K. The intensity ratio of bulk to surface features however was always less favourable than in the case of the broken sample.

An inspection of the curves of Fig. 2 reveals that the observed evolution is incompatible with the simple thermal broadening of a conventional one-electron spectral feature. In fact, the temperature dependence of the Fermi function could not affect the total integrated spectral weight, whose constant value reflects the conservation of the number of particles. The integrated spectral weight is clearly not conserved in the spectra of Fig. 2, where the large loss of peak intensity is not compensated by the tail extending beyond $E_F$. This proves that the usual temperature dependence of a metallic one-particle density of states is inappropriate to explain the experimental result.

To the best of our knowledge only the Anderson model offers a natural explanation for the temperature dependence of the spectral weight. At $T=0$ the Kondo resonance at binding energy $k_B T_K$ reflects the formation of the singlet ground state with a $4f$ occupancy $n_f=14-n_h$ ($n_h=1$ for an unhybridized $4f^{13}$ Yb ion). At $T\neq 0$ low-lying magnetic states ($n_h=1$) are thermally populated and the average hole number $\langle n_h\rangle$ increases, as does the effective valence. The temperature dependence of the Kondo resonance follows that of $(1-\langle n_h\rangle)$, so that its integrated intensity is strongly reduced when the temperature varies from well below to well above the Kondo temperature [4]. When a nonzero crystal field interaction partially lifts the degeneracy of the $4f_{7/2}$ manifold, the spectral intensity is distributed between the Kondo resonance and crystal field excited levels. The explicit temperature dependence of $\langle n_h\rangle$ is somewhat modified from the previous case, but the integrated weight of the Kondo resonance and of its CEF satellites still follows $(1-\langle n_h\rangle)$, and a reduction is expected with increasing temperature. The temperature dependence observed in Fig. 2 is therefore not only qualitatively consistent with, but is required by the Anderson model.

To test whether the predictions of the Kondo model are also quantitatively consistent with the experimental results of Fig. 2 we have performed a temperature dependent calculation of the $4f$ spectral function, within the non-crossing approximation (NCA) of the Anderson model [4]. The parameters of our calculation were, in the notation of [7], $\varepsilon_f=-0.3$ eV, $\Delta=0.015$ eV (the hybridization strength), a spin orbit splitting $\Delta_{so}=1.4$ eV, $U=\infty$ ($n_h=0,1$ basis states). The level scheme was that of [19], with a $\Gamma_7$ ground state doublet and $\Gamma_8$ ($N=4$) and $\Gamma_6$ ($N=2$) CEF excited states at 4 meV and 7 meV. The Kondo temperature corresponding to these parameters was 65 K, in agreement with the estimated value $T_K=60$ K of [19]. Our calculation essentially reproduces the results of Bickers, Cox and Wilkins (Fig. 34 of [4]). We obtain a sharp peak, consisting of the Kondo resonance and CEF excited states, at 8 meV with a total width of 15 meV at 20 K. Both the position and the width of this feature are underestimated by the calculation. We shall discuss this shortcoming of the model in a subsequent paragraph. At this point, however, we concentrate on the temperature dependence of the spectral weight. The calculated integrated intensity of the shallower peak, arbitrarily nor-

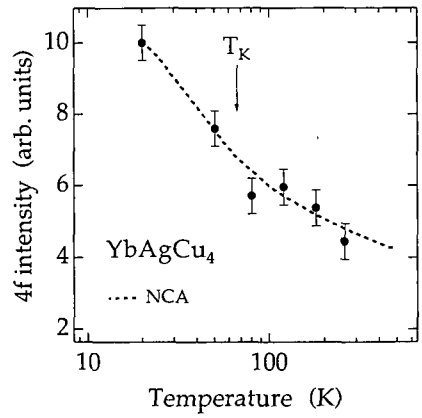


**Fig. 3.** Calculated (dashed line) and experimental (solid symbols) integrated intensity of the Kondo peak. The NCA calculation, performed for a Kondo temperature $T_K=65$ K and a doublet CEF ground state, corresponds to a change of Yb valence from 2.88 at 20 K to 2.95 at 500 K. The experimental values have been obtained by integrating the spectra of Fig. 2 after subtraction of the contribution from a flat non-$f$ density of states. The theoretical and experimental values have been arbitrarily normalized to 10 at 20 K

malized to 10 at 20 K, is reproduced in Fig. 3. It reflects the temperature evolution of the term $(1-\langle n_h \rangle)$ which varies from 0.12 at 20 K to 0.05 at 500 K. The theoretical curve is compared with the experimental integrated $4f$ signal. This is obtained at each temperature by integrating the spectra of Fig. 2, after subtraction of the step-like contribution from band states. The experimental values have also been scaled to a value of 10 at 20 K, and the error bars represent an estimation of the maximum error involved in the procedure of normalization and subtraction of the non-$f$ contribution. The agreement between theory and experiment, and the disagreement with the temperature-independent integrated intensity expected for a normal metal are striking. A similar calculation performed with $T_K = 150$ K and no CEF splitting would yield a somewhat worse, although qualitatively good, agreement. At this stage, however, we are reluctant to attach too much importance to such subtle effects. The important physical message conveyed by Fig. 3 is that the spectral function evolves significantly on a temperature scale set by $T_K$, as predicted by the Anderson model.

The observation of an evolution controlled by $T_K$ confirms our previous BIS results on $CePd_3$ [10] and $CeSi_2$ [11], and definitely establishes the existence of a characteristic temperature scale in the spectral properties of Ce and Yb compounds. An independent confirmation comes from recent X-ray absorption data of the Yb $L_3$ edge in $YbAgCu_4$, that reveal a temperature induced change of Yb $4f$ occupancy completely consistent with our estimation [21]. These experimental results strongly support the Kondo picture. However, keeping this success in mind, one should not ignore the fact that the agreement between calculated and experimental spectra is far from perfect. The experimental $4f$ feature of Fig. 2 is in fact substantially broader and the peak too far from $E_F$ than predicted by the model, even when CEF satellites are taken into account. Our calculation for $YbAgCu_4$ yields a 15 meV wide peak centered at $\sim 8$ meV, while the experimental peak position is 25 meV. We notice however that in spectra of $YbAgCu_4$ collected with a resolution of 60 meV the maximum of the Kondo peak is observed at 60 meV [13]. We notive also that in high resolution spectra of more strongly hybridized Yb compounds, the Kondo peak is found as far as $\sim 45$ meV [22]. We must conclude that the model underestimates the experimental binding energy of the peak, but that the latter is certainly not invariant as suggested [13], and is probably mainly determined by the experimental resolution.

Since the experimental and thermal broadening have a negligible effect on the position of the sharp calculated Kondo peak, our observations suggest that the spectral feature is intrinsically asymmetric and broader than the calculated one. The combined effect of a tail on the high binding energy side, and of the experimental broadening, could therefore be the single cause of the discrepancies between the calculated and observed lineshape. At the present time one can only speculate on the origin of this asymmetric broadening which is clearly not included in the model. Takeshige et al. [23] have considered for instance the effect of an additional repulsive term describing $d-f$ Coulomb interaction, and found a substantial broadening of the spectral features. On the other hand broadening mechanisms inherent to the photoemission process itself could play an important role in determining the width of the Kondo peak. The example of Yb is emblematic because the bulk $4f$ signal near $E_F$ is well separated from the surface contribution. Before escaping into the vacuum photoelectrons generated in the bulk must necessarily diffuse through the surface layer, where they can lose energy to phonons or electron-hole excitations. These scattering processes define a finite photoelectron lifetime which, combined with the hole lifetime, determine the total photoemission linewidth [24]. One can anticipate that systematic high-resolution measurements performed with variable probing depth at different photon energies, or even with overlayers of variable thickness to control the amount of scattering, could greatly contribute to elucidate this delicate point.

Is the discrepancy between theory and experiment sufficiently serious to rebut the Kondo scenario for the spectroscopic data? In our opinion, the answer is definitely no. The model is not only clearly successful in describing thermodynamic properties. When the entire $4f$ signal can be unambiguously extracted from the experimental data [25], it also correctly predicts the relative intensities of the various spectral features. Moreover, as discussed throughout this paper, the temperature dependence represents a fundamental aspect of the model, since it reflects the scaling behavior of the Kondo phenomenology and the progressive evolution from a local Fermi liquid ground state to a localized moment regime. Such a temperature dependence simply cannot be explained by usual one-particle approaches valid for weakly correlated metals. Compared to this crucial prediction, the poor fit to the observed lineshape should rather be regarded as a minor point that needs to be clarified. Efforts towards a more realistic description of the photoemission process should obviously be strongly encouraged.

We gratefully acknowledge the assistance of G. Schmerber in the sample preparation and characterization. We also thank Dr. L.H. Tjeng for making available to us his unpublished results. This paper has been supported by the Fonds National Suisse de la Recherche Scientifique.

## References

1. Lawrence, J.M., Riseborough, P.S., Parks, R.D.: Rep. Prog. Phys. **44**, 1 (1981)
2. Lee, P.A., Rice, T.M., Serene, J.W., Sham, L.J., Wilkins, J.W.: Comments Condensed Matter Phys. **12**, 99 (1986)
3. Gunnarsson, O., Schönhammer, K.: Phys. Rev. B**28**, 4315 (1983)
4. Bickers, N.E., Cox, D.L., Wilkins, J.W.: Phys. Rev. B**36**, 2036 (1987)
5. Fuggle, J.C., Hillebrecht, F.U., Zolnierek, Z., Lässer, R., Freiburg, Ch., Gunnarsson, O., Schönhammer, K.: Phys. Rev. B**27**, 7330 (1983)
6. Allen, J.W., Oh, S.J., Gunnarsson, O., Schönhammer, K., Maple, M.B., Torikachvili, M.S., Lindau, I.: Adv. Phys. **35**, 275 (1986)
7. Patthey, F., Imer, J.-M., Schneider, W.-D., Beck, H., Baer, Y., Delley, B.: Phys. Rev. B**42**, 8864 (1990)
8. Liu, L.Z., Allen, J.W., Gunnarsson, O., Christensen, N.E., Andersen, O.K.: Phys. Rev. B**45**, 8934 (1992)

9. Patthey, F., Schneider, W.-D., Baer, Y., Delley, B.: Phys. Rev. Lett. **58**, 2810 (1987)
10. Malterre, D., Grioni, M., Weibel, P., Dardel, B., Baer, Y.: Phys. Rev. Lett. **68**, 2656 (1992); Phys. Rev. Lett. **69**, 3419 (1992)
11. Malterre, D., Grioni, M., Weibel, P., Dardel, B., Baer, Y.: Europhys. Lett. **20**, 445 (1992)
12. Oh, S.-J.: In: Proceedings of the International Conference on Strongly Correlated Electron Systems, Sendai 1992; to be published in Physica B; Tjeng, L.H.: (Private communication)
13. Lawrence, J.M., Arko, A.J., Joyce, J.J., Canfield, P.C., Fisk, Z., Thompson, J.D., Bartlett, R.J.: J. Magn. Magn. Mater. **108**, 215 (1992); Joyce, J.J., Arko, A.J., Lawrence, J.M., Tang, J., Canfield, P.C., Bartlett, R.J., Fisk, Z., Thompson, J.D.: Solid State Commun. **83**, 551 (1992)
14. Rossel, C., Yang, K.N., Maple, M.B., Fisk, Z., Zirngiebl, E., Thompson, J.D.: Phys. Rev. B**35**, 1914 (1987)
15. Androja, D.T., Malik, S.K., Padalia, B.D., Vijayaraghavan, R.: J. Phys. C**20**, L307 (1987)
16. Besnus, M.J., Haen, P., Hamdaoui, N., Herr, A., Meyer, A.: Physica B**163**, 571 (1990)
17. Severing, A., Murani, A.P., Thompson, J.D., Fisk, Z., Loong, C.-K.: Phys. Rev. B**41**, 1739 (1990)
18. Nakamura, H., Nakajima, K., Kitaoka, Y., Asayama, K., Yoshimura, K., Nitta, T.: Physica **B171**, 238 (1990)
19. Polatsek, G., Bonville, P.: Z. Phys. B**88**, 189 (1992)
20. Kang, J.-S., Allen, J.W., Rossel, C., Seaman, C.L., Maple, M.B.: Phys. Rev. B**41**, 4078 (1990)
21. Lawrence, J.M., Kwei, G.H., Canfield, P.C, Witt, J.G. de: (Preprint)
22. Weibel, P., Malterre, D., Grioni, M., Dardel, B., Baer, Y.: (to be published)
23. Takeshige, M., Sakai, O., Kasuya, T.: J. Magn. Magn. Mater. **52**, 363 (1985)
24. Thiry, P.: Thesis, Université Paris-Sud, 1981 (unpublished)
25. Weibel, P., Malterre, D., Grioni, M., Dardel, B., Baer, Y.: Z. Phys. B**87**, 165 (1992)

# Evidence of a Kondo Scale from the Temperature Dependence of Inverse Photoemission Spectroscopy of $CePd_3$

D. Malterre, M. Grioni, P. Weibel, B. Dardel, and Y. Baer
*Institut de Physique, Université de Neuchâtel, CH-2000 Neuchâtel, Switzerland*
(Received 8 October 1991)

Inverse photoemission spectra have been measured as a function of temperature in $CePd_3$. Although the experimental energy resolution is 1 order of magnitude larger than the characteristic thermodynamic energy scale of this system, a temperature dependence of the spectral function is observed. This result proves that high-energy spectroscopies are sensitive to the breakdown of the Kondo state as the low-lying magnetic states become thermally populated.

PACS numbers: 71.28.+d, 73.20.At, 78.70.En, 79.20.Hx

Electronic correlations play a fundamental role in the physical properties of solids [1,2]. Although weakly correlated systems like simple metals are well described in terms of itinerant electron bands, a localized description becomes more appropriate for strongly correlated materials. Rare-earth systems represent the limiting case of very large intra-atomic Coulomb interactions with atomiclike $4f$ states. However, in several cerium compounds, unusual properties are observed resulting from the competition between the correlations of the $f$ electrons and their hybridization with conduction states [3,4]. At low temperature, these systems behave like Fermi liquids but above a characteristic temperature (the Kondo temperature $T_K$) a progressive evolution to a localized behavior takes place [5]. The Kondo energy ($\delta = k_B T_K$), which represents the splitting between the singlet ground state and the low-lying magnetic states, determines the scaling behavior of the physical properties. For example, the magnetic susceptibility is temperature independent for $T \ll T_K$, it exhibits a broad maximum around $T_K$, and for $T \gg T_K$ it follows a Curie-Weiss law reflecting the formation of a local moment as magnetic excited states become thermally populated.

High-energy spectroscopic techniques are particularly useful in revealing the correlations since their strength is related to the energy positions of satellite structures [6–8]. Nevertheless, such techniques under standard conditions have never revealed the low-energy scale which governs the thermodynamic properties. To the best of our knowledge, the only spectroscopic investigation of the thermal excitations in a Kondo system was the high-resolution photoemission study of $CeSi_2$ [9]. This study showed a temperature dependence of the spectral function just below the Fermi energy ($E_F$). In the framework of the single impurity Anderson model, the intensity at $E_F$ in the photoemission spectrum reflects the tail of the Kondo resonance which develops in the spectral function at energy $\delta$ above $E_F$. This resonance results from the formation of a singlet ground state and it is expected to be strongly reduced as excited magnetic states become thermally populated (for temperatures above $T_K$) [10–12]. This effect in photoemission is subtle and has been recently called into question [13]. However, as the main weight of the Kondo resonance is located above $E_F$, the $N+1$ (electron addition) part of the spectral function, which is probed by bremsstrahlung isochromat spectroscopy (BIS), should be more sensitive to the temperature dependence of the Kondo effect. In this paper we show for the first time that the $4f$ BIS spectral function exhibits an important temperature dependence despite the fact that the state-of-the-art experimental resolution is more than 1 order of magnitude larger than the Kondo energy. This result definitely establishes that high-energy spectroscopies give information on the energy scale responsible for the thermodynamic properties.

$CePd_3$ is a good candidate for this investigation. Previous high-energy spectroscopy experiments [14–17] on this system have shown a significant $4f$ configuration admixture in the ground state. Moreover, resistivity and magnetic measurements [18,19] suggest a Kondo temperature around 240 K. $CePd_3$ has been prepared by arc-melting the constituent materials several times under argon atmosphere. X-ray powder diffraction patterns have confirmed the single phase nature with the $AuCu_3$ structure of the sample. BIS spectra have been obtained with a photon energy of 1486.6 eV and a total energy resolution of 0.6 eV was achieved. The sample could be cooled with a closed-cycle He refrigerator at about 15 K. The pressure was in the low $10^{-10}$-Torr range. Clean samples were obtained by scraping the surface with a diamond file, and the surface cleanliness was regularly checked by photoemission.

Figure 1 shows the BIS spectrum of $CePd_3$ for $T = 15$ and 300 K. The room-temperature spectrum is in good agreement with previously reported data [20,21]. The spectra are dominated by the $4f$ contribution which results in a narrow peak just above the Fermi energy and a broad structure centered at about 5 eV. The additional peak at 2.2 eV was interpreted to be the cerium $5d$ split-off band and it is encountered in many $XPd_3$ compounds ($X$ = rare earth, yttrium) [21,22]. These different features are superimposed to a broad, structureless $sp$ band as clearly illustrated by the BIS spectrum of $YPd_3$ [21]. The intensities of the two spectra have been normalized at the highest energy (8.5 eV) where the $4f$ signal vanishes. In order to isolate the $4f$ excitations, we

 

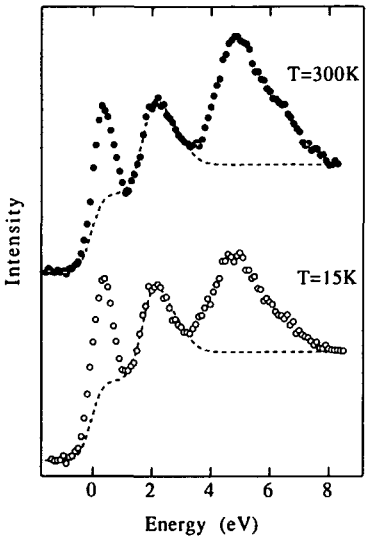


FIG. 1. BIS spectra of the $CePd_3$ compound at $T=15$ K (open circles) and $T=300$ K (solid circles). The dashed lines are the assumed non-$f$ contribution and inelastic background.

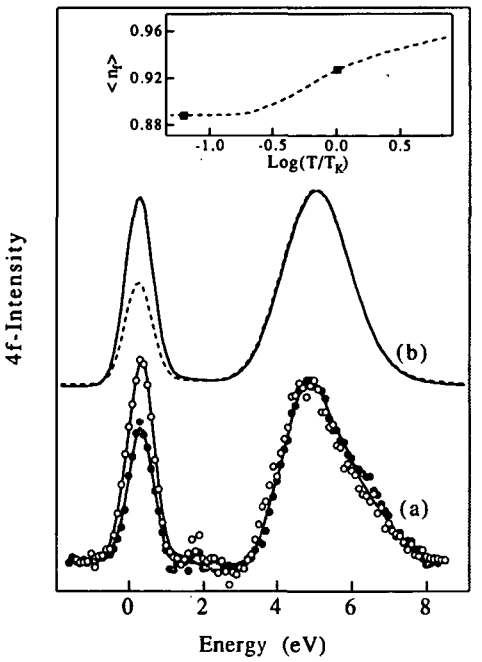


FIG. 2. (a) $4f$-BIS spectral function normalized to the intensity maximum of the high-energy structure for two temperatures $T=15$ K (open circles) and $T=300$ K (solid circles) obtained by removing a background from the experimental spectra. The solid lines are a guide for the eye. (b) Calculated $4f$ spectral function normalized to the intensity maximum of the high-energy structure for $T=0$ K (solid line) and $T=300$ K (dashed line). The peaks near $E_F$ were convoluted by a Gaussian (0.7 eV FWHM) to account for the experimental resolution and the high-energy structure ($4f^2$ final states) was broadened by a Gaussian (2 eV FWHM) to account for the multiplet effect. The $T=0$ K spectrum is calculated in the Gunnarsson-Schönhammer model with the following parameters: $U_{ff}=5.7$ eV, $\varepsilon_f=-1.5$ eV, $\Delta_{s.o.}=2.80$ meV, and $\Gamma=90$ meV. Inset: A NCA calculation of the mean value of the $4f$ occupation number as a function of temperature. The two black squares represent the calculated values of $\langle n_f \rangle$ for $T=15$ and 300 K.

have simulated the contributions of non-$f$ states and of the inelastic background by a simple analytical function (dashed curve in Fig. 1) reproducing the BIS spectrum of $YPd_3$ [21]. We are aware that this procedure is somewhat arbitrary but, for the purpose of demonstrating the temperature evolution of the spectra, the most important point is to assume exactly the same function in both spectra since no mechanism predicts a sizable temperature dependence of these contributions. A simple inspection of the raw data reveals unambiguously that between 15 and 300 K the relative intensity of the two $4f$ features is markedly modified. This is more clearly demonstrated in Fig. 2(a) where the $4f$ intensities obtained from Fig. 1 are reported for the two temperatures and normalized for clarity to the maximum of the high-energy structure.

The presence of well-separated structures in the BIS spectra reflects many-body or dynamical effects and can be easily understood in the framework of the Gunnarsson-Schönhammer (GS) model [8]. The zero-temperature spectrum can be calculated with this variational approach. The BIS spectral function corresponds to transition from the ground state ($N$ particle state) toward the $N+1$ particle excited states. The high-energy structure represents the final states of $4f^2$ character, its position is determined by the intra-atomic Coulomb interaction $U_{ff}$ and the $4f$ energy $\varepsilon_f$. On the other hand, the peak just above the Fermi energy (the $4f^1$ final states) is mainly composed of two contributions: the Kondo resonance at $\delta=k_BT_K$ and the spin-orbit satellite at $E=\delta+\Delta_{s.o.}$ ($\Delta_{s.o.}=280$ meV in cerium) [12]. As a result of the limited experimental resolution of the technique, these two latter structures are not experimentally resolved and only one peak about 0.8 eV wide is observed.

At finite temperature, this picture is modified. As the available final states do not depend on temperature, the variation of the spectral function results from the modification of the initial state: At $T=0$ K, the initial state is the singlet ground state but it becomes a statistical admixture involving multiplet excited states at $T\neq 0$ K. The finite-temperature spectrum cannot be obtained in the GS approach; however, the low-energy peak can be calculated in the noncrossing approximation (NCA) of the infinite $U_{ff}$ degenerate Anderson model [10–12]. In this formalism, a temperature dependence of the spectral function is expected. The low-energy structures, composed of the Kondo and the spin-orbit resonances, are both strongly depleted when the temperature increases from $T\ll T_K$ to $T\gg T_K$. On the contrary, the $N-1$ part of the density of states is less sensitive to temperature effects. The weight of the photoemission spectrum (PES) is nearly constant [23] although the shape near $E_F$ varies with temperature as experimentally shown by the high-resolution photoemission study of $CeSi_2$ [9]. This con-

trasted behavior of PES and BIS spectra results from the different nature of the final states in the two spectroscopies [12]. The structures at $E=\delta$ and $E=\delta+\Delta_{s.o.}$ in the BIS spectrum are associated with $4f^1$ final states with negligible $4f^0$ admixture. As the thermally excited states have also a predominantly $4f^1$ character, the coupling with these $4f^1$ BIS final states, which is determined by the matrix elements $\langle N+1|a_f^\dagger|\Psi_{ex}\rangle$, is negligible. $|\Psi_{ex}\rangle$ is a thermal excited state, $a_f^\dagger$ the creation operator of a $4f$ electron, and $|N+1\rangle$ a final state of BIS. Therefore, the thermal population of the excited states increases only the $4f^2$ peak whereas the corresponding loss of statistical weight of the ground state decreases the $4f^1$ peak. On the other hand, the photoemission final states $|N-1\rangle$ at $E_F$ and $E=-\Delta_{s.o.}$ have a $4f^0$-$4f^1$ admixture similar to that in the ground state and, therefore, the spectral intensity is determined by the weight of the $f^1$ configuration in the initial state and $f^0$ configuration in the final states. As the $f^1$ contributions in the ground and excited states are roughly the same, the spectral weight in photoemission has a much weaker temperature dependence than the BIS part.

In order to simulate the spectral function for finite temperatures and $U_{ff}$, we use a phenomenological procedure. First, we calculate the mean value of the $4f$ occupation number $\langle n_f\rangle$ as a function of temperature in the NCA (inset of Fig. 2). For a Kondo temperature of $T_K=240$ K, $\langle n_f\rangle$ increases from $n_{f,g.s.}=0.89$ at $T\rightarrow 0$ to $\langle n_f\rangle=0.93$ at room temperature. This evolution reflects the progressive population of the low-lying excited states with $n_{f,ex}\approx 1$ as $T$ increases. Then, we determine the respective populations, $a(T)$ and $b(T)$, of the ground and excited states in the initial statistical admixture from the calculated value of the $4f$ occupation number at $T$: $\langle n_f\rangle(T)=a(T)n_{f,g.s.}+b(T)n_{f,ex}$. The finite-temperature spectra are simply calculated from a combination of the BIS spectra corresponding to the ground and excited states weighed by their respective population in the initial state:

$$A(\omega,T)=a(T)A_{GS}(\omega)+b(T)A_{ex}(\omega), \qquad (1)$$

where $A_{GS}(\omega)$ is the $T=0$ K spectrum calculated in the Gunnarsson-Schönhammer model [8] and $A_{ex}(\omega)$ is the calculated spectrum for a $4f^1$ initial state, which only exhibits the high-energy structure corresponding to $4f^2$ final states.

Then, with increasing temperature, there is an intensity transfer from the $4f^1$ to the $4f^2$ peak but, in order to make easier the comparison with experiment, the calculated $4f$ spectral functions have been normalized to the maximum of the $4f^2$ structure [Fig. 2(b)]. The effect of temperature is well described within our simple approach but it is slightly overestimated. Experimental and theoretical arguments could explain the small differences between measured and calculated finite-temperature spectral functions. The presence of the split-off band structure in the BIS spectra prevents a very accurate determination of the $4f$ intensity in the experimental spectra. Moreover, the value of $\langle n_f\rangle$ is calculated in the infinite $U_{ff}$ limit; finite $U_{ff}$ can introduce a slight modification of the $\langle n_f\rangle$ temperature dependence. These small differences can also result from the technique itself. Recently, it has been demonstrated that the cerium valence at the surface in $CePd_3$ is nearly trivalent ($n_f=0.99$) and strongly differs from the bulk value ($n_f=0.85$) [24]. This different valence at the surface mainly results from a modification of the coordination and then should be temperature independent. The surface contribution leads to a reduction of the experimental temperature effect and should be taken into account in an accurate quantitative analysis. Despite these limitations, the BIS spectral function clearly exhibits a temperature dependence revealing unambiguously a Kondo energy scale in the electronic properties. Recently, it was proposed that the $f$ electrons in hybridized systems like $\alpha$-Ce can be described in a one-electron band model [25]. Such temperature-dependent spectroscopic behaviors can hardly be reconciled with a band picture of the $4f$ electrons and then strongly support the description of $f$ states in terms of an impurity many-body model [26].

To summarize, this study shows an indisputable temperature dependence of the spectral function. As the BIS $4f^1$ structure is composed of the Kondo and spin-orbit resonances which are both depleted with increasing temperature through the low-energy scale $T_K$, our measurements show the same progressive evolution from a Fermi liquid to a localized behavior exhibited by near-ground-state properties such as magnetic susceptibility, specific heat, resistivity, etc. As a consequence, the ground-state parameters of the Anderson model, which have been derived from room-temperature XPS or BIS experiments without considering this important temperature effect, will have to be critically reviewed. Our results also demonstrate that even with a resolution 1 or 2 orders of magnitude worse than the low-energy scale ($k_BT_K$), BIS reflects the subtle modification of the initial state with temperature and offers a new tool for the investigation of the unconventional physical properties of hybridized $4f$ systems.

The authors gratefully thank C. Andreani and J. Sorel for discussions and B. Delley who has developed the computer codes for the NCA calculations. This work has been supported by the Fonds National Suisse de la Recherche Scientifique.

[1] P. Fulde, Prog. Theor. Phys. **80**, 47 (1984).
[2] S. Hüfner, in *Photoemission in Solids II*, edited by L. Ley and M. Cardona (Springer-Verlag, Berlin, 1979), Vol. 27, p. 173.
[3] J. M. Lawrence, P. S. Riseborough, and R. D. Parks, Rep. Prog. Phys. **44**, 1 (1981).
[4] P. A. Lee, T. M. Rice, J. W. Serene, L. J. Sham, and J.

W. Wilkins, Comments Condensed Matter Phys. **12**, 99 (1986).
[5] P. Nozières, J. Low Temp. Phys. **17**, 31 (1974).
[6] A. Kotani, in *Handbook of Synchrotron Radiation*, edited by G. V. Marr (Elsevier, Amsterdam, 1987), Vol. 2, p. 611.
[7] J. W. Allen, S. J. Oh, O. Gunnarsson, K. Schönhammer, M. B. Maple, M. S. Torikachvili, and I. Lindau, Adv. Phys. **35**, 275 (1986).
[8] O. Gunnarsson and K. Schönhammer, Phys. Rev. B **28**, 4315 (1983).
[9] F. Patthey, W.-D. Schneider, Y. Baer, and B. Delley, Phys. Rev. Lett. **58**, 2810 (1987).
[10] H. Kojima, Y. Kuramoto, and M. Tachiki, Z. Phys. B **54**, 293 (1984).
[11] N. Grewe, Z. Phys. B **53**, 271 (1983).
[12] N. E. Bickers, D. L. Cox, and J. W. Wilkins, Phys. Rev. Lett. **54**, 230 (1985); Phys. Rev. B **36**, 2036 (1987).
[13] J. Joyce, A. J. Arko, R. J. Bartlett, C. Canfield, Z. Fisk, J. Lawrence, and J. Tang, Bull. Am. Phys. Soc. **36**, 460 (1991).
[14] F. U. Hillebrecht, J. C. Fuggle, G. A. Sawatzky, M. Campagna, O. Gunnarsson, and K. Schönhammer, Phys. Rev. B **30**, 1777 (1984).
[15] J. C. Fuggle, F. U. Hillebrecht, Z. Zolnierek, R. Lässer, Ch. Freiburg, O. Gunnarsson, and K. Schönhammer, Phys. Rev. B **27**, 7330 (1983).
[16] E. Wuilloud, W.-D. Schneider, B. Delley, Y. Baer, and F. Hullinger, J. Phys. C **17**, 4799 (1984).
[17] R. D. Parks, S. Raen, M. L. denBoer, V. Murgai, and T. Mihalisin, Phys. Rev. B **28**, 3556 (1983).
[18] J. M. Lawrence, J. D. Thompson, and Y. Y. Chen, Phys. Rev. Lett. **54**, 2537 (1985).
[19] J. Aarts, F. R. deBoer, P. F. de Châtel, and A. Menovsky, Solid State Commun. **56**, 623 (1985).
[20] Y. Baer, H. R. Ott, J. C. Fuggle, and L. E. De Jong, Phys. Rev. B **24**, 5384 (1981).
[21] F. U. Hillebrecht, J. C. Fuggle, G. A. Sawatzky, and R. Zeller, Phys. Rev. Lett. **51**, 1187 (1983).
[22] C. Koenig and M. A. Khan, Phys. Rev. B **38**, 5887 (1988).
[23] O. Gunnarsson and K. Schönhammer, in *Handbook on the Physics and Chemistry of Rare-Earths*, edited by K. A. Gschneidner, Jr., L. Eyring, and S. Hüfner (North-Holland, Amsterdam, 1987), Vol. 10, p. 103.
[24] C. Laubschat, E. Weschke, C. Holtz, M. Domke, O. Stebel, and G. Kaindl, Phys. Rev. Lett. **65**, 1639 (1990).
[25] O. Eriksson, R. C. Albers, A. M. Boring, G. W. Fernando, Y. G. Hao, and B. R. Cooper, Phys. Rev. B **43**, 3137 (1991).
[26] Y. Baer, M. Grioni, D. Malterre, and W.-D. Schneider, Phys. Rev. B **44**, 9108 (1991).

PHYSICAL REVIEW B VOLUME 48, NUMBER 14 1 OCTOBER 1993-II

# Correlation between the Kondo temperature and the photoemission spectral function in the $CeSi_x$ ($1.6 \leq x \leq 2$) system

D. Malterre, M. Grioni, P. Weibel, B. Dardel, and Y. Baer
*Institut de Physique, Université de Neuchâtel, CH-2000 Neuchâtel, Switzerland*
(Received 1 February 1993; revised manuscript received 28 July 1993)

In this paper, we study the evolution of the photoemission $4f$-electron spectral density as a function of concentration in the $CeSi_x$ ($1.6 \leq x \leq 2$) system. The physical properties are strongly composition dependent around $x = 2$ reflecting large variations of the Kondo temperature with Si vacancies. Then this system represents an ideal case for photoemission investigations since it is possible to tune the Kondo temperature without significant changes of the non-$f$-electron density of states. Our spectroscopic measurements show a correlation between the Kondo temperature and the $4f$ intensity near the Fermi level as expected in the framework of the single-impurity Anderson model.

In the last decade, numerous studies using high-energy spectroscopies have given fruitful information on the $4f$ states in cerium-based heavy-fermion systems.[1,2] In particular, high-resolution $4f$ photoemission spectra exhibit the different energy scales corresponding to charge fluctuations, spin orbit, and crystal-field excitations expected from the single-impurity Anderson model (SIAM).[3] However, a recent resonant photoemission study of several Ce heavy fermion compounds claims that the $4f$ spectrum reveals several inconsistencies with the predictions of the SIAM:[4] (i) the width of the feature near $E_F$ resulting from the Kondo resonance and its crystal-field sideband is too broad; (ii) no temperature dependence of the Kondo resonance is observed; (iii) there is no correlation between the spectral weight near $E_F$ and the Kondo temperature. The suitability of the SIAM to describe the spectroscopic properties is then called into question. Our recent studies challenge this conclusion at least concerning the temperature dependence of the spectral density.[5,6] As the Kondo resonance is located above $E_F$ in Ce compounds, we have investigated the evolution of the inverse photoemission spectra with temperature and we have shown that the $4f$ spectral density exhibits a temperature dependence reflecting the smearing of the Kondo resonance when temperature is larger than $T_K$. In this Rapid Communication, we investigate the third alleged inconsistency and demonstrate that there is an actual relation between the spectral weight near $E_F$ and the Kondo temperature. In general, a quantitative study of this effect is difficult to perform because, even with $4f$ resonant photoemission, the states of other symmetries strongly contribute to the photoemission spectra and may prevent an accurate determination of the $4f$ signal. In order to avoid these difficulties, we have chosen to measure several $CeSi_x$ alloys. While the non-$f$ spectral weight is expected to be weakly affected by the concentration of Si vacancies, the physical properties associated with the $f$ states are known to be strongly composition dependent in this system.[7-10] $CeSi_2$ is a well-known heavy fermion with a nonmagnetic ground state corresponding to a Kondo temperature ($T_K$) estimated between 35 and 100 K; below $x = 1.80$ a ferromagnetic order appears around 10 K with a reduced magnetic moment, suggesting that the Kondo temperature drops with decreasing Si content.[6,7,11,12] Therefore, this system is especially appropriate to determine the modification of the *4f spectral density* accompanying the change of $T_K$.

$CeSi_x$ ($1.6 \leq x \leq 2$), $LaSi_2$, and $CeGe_2$ samples were made by arc melting the constituent materials several times under argon atmosphere and they were characterized by x-ray powder diffraction patterns and magnetic measurements. $CeSi_2$ which crystallizes in the tetragonal $\alpha$-$ThSi_2$ structure, admits a considerable amount of vacancies on the Si sublattice ($x \geq 1.75$) while still retaining its tetragonal symmetry.[9] Below $x = 1.75$ a distortion occurs and the alloys have the $\alpha$-$GdSi_2$-type structure but this structural modification does not markedly affect the electronic and physical properties of the alloys.[9,10] The different spectroscopic measurements were performed in an apparatus combining ultraviolet photoemission spectroscopy (UPS), x-ray photoemission spectroscopy (XPS), and bremsstrahlung isochromat spectroscopy (BIS). The sample could be cooled with a closed-cycle He refrigerator to about 15 K. In UPS the overall energy resolution, estimated from the width of the Fermi step, is better than 20 meV. BIS spectra were obtained with a photon energy of 1486.6 eV and a total energy resolution of 0.6 eV was achieved. The pressure was in the low $10^{-10}$ Torr range during the measurements. The samples were cleaned by repeated scraping with a diamond file until no oxygen contamination (O $1s$ and O $2p$ photoemission signals) could be detected.

In Fig. 1, we report the He II ($h\nu = 40.8$ eV) photoemission (UPS) and inverse photoemission (BIS) spectra of $CeSi_2$ and $CeSi_{1.6}$. These spectra exhibit the characteristic features of the Ce-based heavy fermion compounds.[2] The UPS spectra are dominated by a broad structure near $E = -2.5$ eV reflecting the non-$f$ valence-band states and the ionization peak of the Ce atoms ($4f^0$ final state). Near the Fermi level, the two additional well-resolved structures are predicted by the SIAM: the first one just below the Fermi level is interpreted as the tail of the Kondo resonance and the crystal-field excitations whereas the structure near $E = -0.3$ eV corresponds to

0163-1829/93/48(14)/10599(3)/$06.00  

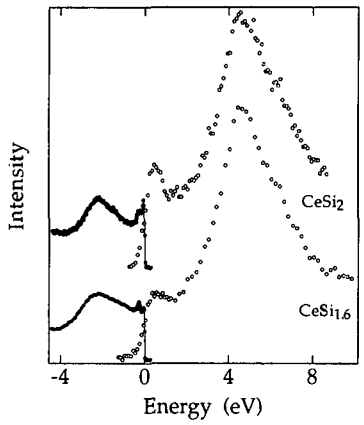


FIG. 1. He II photoemission and inverse photoemission spectra for $CeSi_2$ and $CeSi_{1.6}$ at $T=15$ K.

the spin-orbit sideband.[3] In the BIS part, the structure located just above $E_F$ represents the Kondo peak and its spin-orbit replicate (not resolved because of the poor BIS energy resolution) and the intense and broad feature between 4 and 7 eV reflects the multiplets of the $4f^2$ final state. In a hypothetical purely trivalent system, only the high-energy features ($E=-2.5$ eV in photoemission spectroscopy and $E=4-7$ eV in BIS) corresponding to $4f^0$ and $4f^2$ final states, would be observed. Then, the spectral weight near $E_F$ reflects the deviation from the trivalency and is roughly proportional to $T_K$.[13-15] The decrease of the near-$E_F$ structures, clearly observed in both spectroscopies when lowering the Si concentration from 2 to 1.6, is fully consistent with the evolution of the Kondo temperature in the $CeSi_x$ system[7,10,11] and with the prediction of the Anderson model.

The quantitative comparison of experimental and theoretical spectra would require a very accurate determination of the $f$ contribution. The extraction of the photoemission $4f$ signal is a notoriously difficult problem in Ce systems, especially for the $4f^0$ structure which is very often obscured by non-$f$ states. This is clearly illustrated in the Fig. 2 where comparison of $CeSi_2$ and $LaSi_2$ spectra shows that the Si derived $sp$ band strongly overlaps the $4f$ contribution in the $-1$, $-3.5$ eV range. Since an accurate estimation of the $f^0$ structure is difficult, we shall focus our attention on the near $E_F$ region (600 meV) and we shall discuss the evolution with composition of the spectra in this region. As $LaSi_2$ exhibits a structureless spectrum in this energy range (cf., Fig. 2), the two observed near-$E_F$ structures in the different $CeSi_x$ alloys can be unambiguously attributed to $f$ states.

Before presenting the composition dependence of the experimental spectra and their correlation to the Kondo temperature, we briefly recall the prediction of the SIAM. Noncrossing approximation (NCA) calculations of the spectral density in the infinite Coulomb interaction limit ($U_{ff}=\infty$) predict that the intensity of the Kondo resonance scales with $T_K$.[14] It has also been shown that, even with crystal-field interactions, the calculated intensity ratio between the structure near the Fermi level and the spin-orbit sideband varies with $T_K$.[3] As recently demonstrated,[16] a finite $U_{ff}$ does not substantially modify this picture so that the near-$E_F$ region should reflect the modification of the physical properties. In Fig. 3, we have reported raw photoemission spectra of $CeSi_2$, $CeGe_2$, and several $CeSi_x$ alloys measured at 15 K with $h\nu=40.8$ eV. The corresponding spectra recorded at $h\nu=21.2$ eV where the $4f$ cross section is strongly reduced do not show any evolution with composition. With decreasing Si content, the intensity of the shallower structure strongly decreases between $x=2$ and $x=1.75$ and saturates for smaller concentration whereas the $-0.3$-eV feature is weakly affected. In $CeGe_2$, the spectral weight associated with the Kondo resonance is not detectable but the intensity of the spin-orbit sideband remains significant. The photoemission data therefore indicate that the Ce ions are not purely trivalent in this material. This is not surprising because although $CeGe_2$ orders magnetically at 7 K with a nonreduced magnetic moment, specific-heat measurements show that the entropy at the transition temperature is slightly less than $R$ ln2, suggesting a residual Kondo effect.[17] The progressive evolution of the $4f$ spectral density with composition is consistent with the prediction of the SIAM. In order to establish this correlation in a more quantitative way,

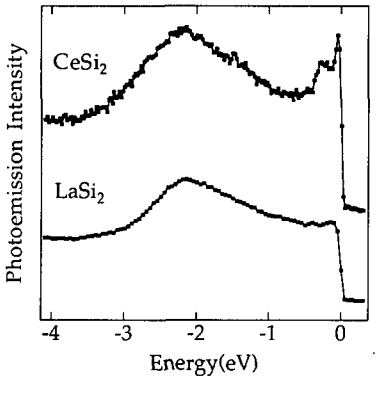


FIG. 2. He II photoemission spectra of $CeSi_2$ and $LaSi_2$ at $T=15$ K.

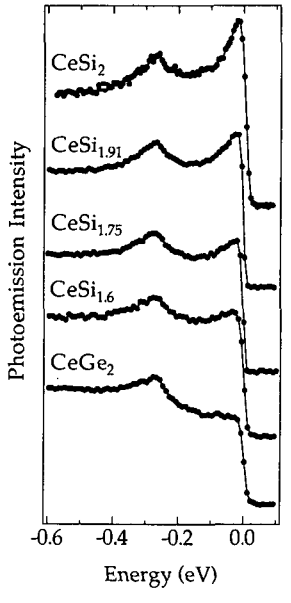


FIG. 3. High-resolution He II spectra at 15 K of the near-$E_F$ region for several alloys of the $CeSi_x$ system and for $CeGe_2$.

we have estimated the intensity ratio between the structure near $E_F$ and its spin orbit sideband as follows. The experimental spectra were fitted by superimposing two Lorentzians simulating the two $4f$ structures on a constant function representing the non-$f$ states. The resulting curves were multiplied by a Fermi function. The phenomenological quantity plotted on the left-hand side of Fig. 4 is the intensity ratio of the two Lorentzians. We also report on the right-hand part of this figure the paramagnetic Curie-Weiss temperature ($\theta_p$), estimated from the temperature dependence of the magnetic susceptibility in Ref. 10, which is known to be proportional to the Kondo temperature. A very good correlation between these two quantities is observed. The possible stabilization of more localized $4f$ states at the surface, recently observed in several cerium-based compounds,[18] could reduce the correlation between Kondo temperature and spectral weight. However the nearly quantitative agreement of estimations of $T_K$ from photoemission and bulk techniques in $CeSi_2$ suggests that this surface effect is less prominent than in strongly hybridized materials like $CeIr_2$ or $CePd_3$ and can be ignored in the present $CeSi_x$ system. The evidence of a scaling between spectroscopic measurements and $T_K$ contrasts with the results of Joyce *et al.*[4] which suggest that the $4f$ spectral weight is not correlated to the value of $T_K$. This discrepancy is a matter of debate and one could speculate that such a behavior could result from the difficulties to extract the $4f$ contribution and then to quantitatively compare $4f$ spectral weight in several materials with very different non-$f$ density of states. Our results establish that, when the variation of the $4f$ signal near $E_F$ can be extracted without ambiguity, it qualitatively scales with $T_K$ in heavy-fermion compounds as expected from the Anderson model.

In this paper, we have investigated the modification of the photoemission spectral density as a function of composition in the $CeSi_x$ system. We show that the intensity of the near-$E_F$ structure which partly reflects the tail of the Kondo resonance, strongly decreases with the concentration of Si vacancies and we verify the correlation between the relative intensity of the two near $E_F$ $4f$ structures and the Kondo temperature. In contrast to recent claims,[4] our results unambiguously show that the evolution of the $4f$ spectra weight near $E_F$ follows, at least qualitatively, the prediction of the Anderson model. To be more quantitative, an accurate determination of the whole $4f$ contribution is required to be compared with calculations of the $4f$ spectral densities. Efforts in this direction are in progress.

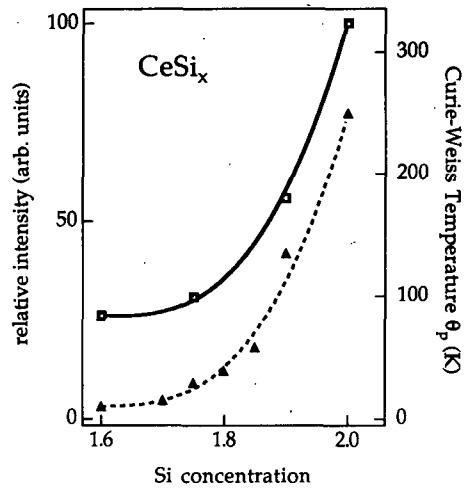


FIG. 4. Left-hand side (black squares): intensity ratio of the two Lorentzians (their widths are kept constant in the series) simulating the near-$E_F$ structures; the solid line is a guide for the eye. Right-hand side (black triangles): evolution of the paramagnetic Curie-Weiss temperature ($\theta_p$) as a function of stoichiometry from Ref. 10; the dashed line is a guide for the eye.

We thank J. Hubsch (service commun de magnétisme de l'Université de Nancy I) for his magnetic measurements. This work was initiated during a visit in the group of F. Girardet (Crissier), whose hospitality is gratefully acknowledged.

[1] *Handbook on the Physics and Chemistry of Rare-Earths*, edited by K. A. Gschneidner, Jr., L. Eyring, and S. Hüfner (North-Holland, Amsterdam, 1987), Vol. 10, p. 103.

[2] J. W. Allen, S. J. Oh, O. Gunnarsson, K. Schönhammer, M. B. Maple, M. S. Torikachvili, and I. Lindau, Adv. Phys. **35**, 275 (1986).

[3] F. Patthey, J. M. Imer, W.-D. Schneider, H. Beck, Y. Baer, and B. Delley, Phys. Rev. B **42**, 8864 (1990).

[4] J. J. Joyce, A. J. Arko, J. Lawrence, P. C. Canfield, Z. Fisk, R. J. Bartlett, and J. D. Thompson, Phys. Rev. Lett. **68**, 236 (1992).

[5] D. Malterre, M. Grioni, P. Weibel, B. Dardel, and Y. Baer, Phys. Rev. Lett. **68**, 2656 (1992); Phys. Rev. Lett. **69**, 3418 (1992).

[6] D. Malterre, M. Grioni, P. Weibel, B. Dardel, and Y. Baer, Europhys. Lett. **20**, 445 (1992).

[7] H. Yashima, H. Mori, T. Satoh, and K. Kohn, Solid State Commun. **43**, 193 (1982).

[8] H. Yashima, T. Satoh, H. Mori, D. Watanabe, and T. Ohtsuka, Solid State Commun. **41**, 1 (1982).

[9] W. H. Lee, R. N. Shelton, S. K. Dhar, and K. A. Gschneidner, Jr., Phys. Rev. B **35**, 8523 (1987).

[10] S. A. Shaheen and J. S. Schilling, Phys. Rev. B **35**, 6880 (1987).

[11] R. M. Galera, A. P. Murani, and J. Pierre, Physica B **156&157**, 801 (1989).

[12] F. Patthey, W.-D. Schneider, Y. Baer, and B. Delley, Phys. Rev. Lett. **58**, 2810 (1987).

[13] O. Gunnarsson and K. Schönhammer, Phys. Rev. B **28**, 4315 (1983).

[14] N. E. Bickers, D. L. Cox, and J. W. Wilkins, Phys. Rev. Lett. **54**, 230 (1985); Phys. Rev. B **36**, 2036 (1987).

[15] N. Grewe, Z. Phys. B **53**, 271 (1983).

[16] J. J. Joyce, A. J. Arko, P. S. Riseborough, P. C. Canfield, J. M. Lawrence, R. I. R. Blyth, R. J. Bartlett, J. D. Thomspon, and Z. Fisk, Physica B **186-188**, 31 (1993).

[17] H. Mori, H. Yashima, and N. Sato, J. Low Temp. Phys. **58**, 513 (1985).

[18] C. Laubschat, E. Weschke, C. Holtz, M. Domke, O. Strebel, and G. Kaindl, Phys. Rev. Lett. **65**, 1639 (1990).

To appear in Rev. Sci. Instrum. 66, July 1995

# A soft x-ray spectrometer for resonant inverse photoemission

P. Weibel, M. Grioni, C. Hêche, and Y. Baer
*Institut de Physique, Université de Neuchâtel, CH2000 Neuchâtel, Switzerland*

(Received 7 February 1995; accepted for publication 14 April 1995)

We describe the concept and the performances of a new tunable soft x-ray inverse photoemission (IPES) spectrometer. The instrument is based on a variable-geometry Bragg spectrograph, and it can be operated with minor modifications over a wide range of photon energies ($600<h\nu<4000$ eV). It was originally designed for IPES measurements of cerium compounds at the Ce $M_5(3d_{5/2}\rightarrow 4f, h\nu=883$ eV) absorption edge, where the Ce $4f$ IPES cross section is resonantly enhanced. Such resonant IPES (RIPES) spectra, now routinely performed by this instrument, are 10–100 times more sensitive to the Ce $4f$ states than conventional x-ray bremsstrahlung spectra, with a comparable energy resolution ($\Delta E\sim 600$ meV). We plan to exploit the wide tunability of the spectrometer to perform RIPES measurements of other correlated materials, namely at the Cu $L_{2,3}(2p\rightarrow d, h\nu=930$ and 950 eV) edge in the high-$T_c$ superconductors. © *1995 American Institute of Physics.*

## I. INTRODUCTION

Inverse photoemission (IPES) is a spectroscopic technique based on the spectral analysis of the photons emitted when a specimen is bombarded with a monochromatic electron beam. Its origins are remote,[1,2] but only in the last two decades has IPES been recognized as a powerful tool for the investigation of the electronic structure of materials. Inverse photoemission is deeply related (by time-inversion symmetry) and complementary to photoelectron spectroscopy (PES).[3] In rather general terms, it can be stated that PES and IPES probe, respectively, the occupied and the unoccupied electron states of a solid.[4] Especially in correlated materials, the combination of PES and IPES yields invaluable information, for instance on the nature and the value of the charge gap in the transition metal oxides,[5] or on the Coulomb correlation energy in rare earths materials.[6] In the much studied mixed-valent cerium compounds, the IPES spectral function provides a direct image of the peculiar low-energy excitations associated with the partially localized $4f$ electrons.[7]

Despite this complementarity, inverse photoemission is not nearly as popular as its direct counterpart. One of the main obstacles to a more widespread use of IPES is its intrinsically low intensity. A simple phase space argument shows in fact that, at a given excitation energy, the IPES cross section is orders of magnitude smaller than the PES cross section.[3] IPES measurements therefore require, especially in the x-ray domain, long acquisition times (typically several hours). Potentially interesting experiments on reactive surfaces and adsorbates at submonolayer coverages are essentially impossible because of the combination of low intensity and reactivity. This limitation is particularly severe for rare earth materials, where even moderate levels of surface contamination can substantially modify the physical properties. These considerations, and our ongoing interest in the electronic structure of cerium-based Kondo systems, have originally motivated our search for an alternative and more effective experimental approach to IPES.

## II. RESONANT INVERSE PHOTOEMISSION

The intensity problem can be tackled by exploiting characteristic features of the energy-dependent cross section. This approach is well known in photoemission. It is based on the observation that, in materials with partially filled and sufficiently narrow bands, transition rates may be selectively enhanced when the excitation energy approaches an appropriate core absorption edge. The quantum interference between direct and indirect transition channels may then produce a resonant enhancement of the photoionization cross section.[8,9]

By analogy with photoemission, resonances can be expected to occur also in IPES. In the usual (or direct) IPES process an incoming free electron undergoes a radiative transition to an empty electronic state. In a rare earth (re) system, for example, the direct IPES transition involving the $4f$ subshell or the re ion is: $4f^n+e^-\rightarrow 4f^{n+1}+h\nu$. When the energy of the incoming electron equals the excitation threshold of a $3d$ or $4d$ core level (as imposed by dipole selection rules) a new indirect channel is opened: $4f^n+e^-\rightarrow \underline{c}4f^{n+2}\rightarrow 4f^{n+1}+h\nu$. The direct and indirect processes have the same initial and final states. They can therefore interfere, and the intensity for the transition $4f^n+e^-\rightarrow 4f^{n+1}+h\nu$ can be selectively and resonantly amplified.

The occurrence of resonances in IPES was demonstrated by pioneering experiments at the $M_{4,5}(3d\rightarrow 4f)$ absorption edges of La and Ce,[10,11] at the $L_{2,3}(2p\rightarrow 3d)$ edges of Ni,[12] and later at the $N_{4,5}(4d\rightarrow 4f)$ absorption edges of the rare earths elements in oxide samples.[13] Those measurements represent remarkable but isolated achievements, and resonant inverse photoemission was essentially abandoned. Today the experimental possibilities have evolved, and the interest for such measurements has grown. In the field of Ce valence fluctuators, for instance, the increased sensitivity of resonant (IPES) (RIPES) to the $4f$ electrons could be exploited to put to a more stringent test prevailing theories for these materials, and the impact should be analogous to that of resonant PES.[7] One can similarly identify, in the physics of the

 0034-6748/95/66(7)/1/7/$6.00  

mixed-valent uranium compounds and of the superconducting cuprates, outstanding problems that could profit from the advantages offered by RIPES. Therefore we set out to design a versatile instrument to perform resonant IPES measurements, which satisfies stringent ultrahigh vacuum (UHV) requirements, and exploits recent technical progress in the handling and detection of soft x rays.

## III. THE RIPES SPECTROMETER

### A. General considerations

An inverse photoemission experiment can be performed in two alternative ways. In the so-called fluorescence mode, and IPES spectrum is obtained at constant electron kinetic energy, by performing a spectral analysis of the emitted photons beam. In the isochromat mode, on the other hand, the emitted intensity is measured at a fixed photon energy, as a function of the electron energy. Both acquisition modes are used in the UV range, while x-ray instruments normally operate in the isochromat mode (hence the historical name of bremsstrahlung isochromat spectroscopy, or BIS). The two modes are usually considered equivalent because, in normal circumstances, changes of the IPES cross section can be neglected over the relevant range of electron energies. Near a resonance, however, this assumption is not valid, and the isochromat mode is unsuitable. A RIPES spectrometer must therefore operate in the fluorescence mode, and accumulate a complete IPES spectrum at each chosen electron energy. In a typical RIPES experiment a large collection of spectra are recorded for different electron energies covering a sufficiently wide range around a selected characteristic threshold (resonance energy). The optical system must therefore accept a correspondingly wide range of photon energies. Moreover, the design must provide the possibility of a broader tuning of the optical system, allowing the instrument to reach other absorption edges of interest.

Resonances of the $4f$ cross section in cerium materials are expected at the $4d$ (BE=120 eV, the usual choice for RESPES) or the $3d$ (BE=883 eV) absorption edges. Apart from any physical considerations, the choice of the most appropriate edge for a RIPES experiment is influenced by technical factors. The handling of photon energies around 120 eV requires a grazing incidence grating monochromator. Such instruments can provide large resolving powers, but require expensive precision-machined gratings, tight mechanical tolerances, and demand a fully windowless vacuum apparatus.[14,15] Also, the small acceptance angles and consequently low transmission of these instruments are possibly incompatible with the low intensity levels of IPES. At higher photon energy, on the other hand, it is possible to take advantage of the intrinsically high resolution, and simpler mechanical design of crystal monochromators. We therefore judged that the choice of the $3d$ edge was preferable. Bragg monochromators based on natural beryl, a beryllium aluminum silicate $[(Be_3Al_2(SiO_3)_6]$, with a distance $2d=15.95$ Å between the $(10\bar{1}0)$ crystalline planes, have been used in this energy range for space and synchrotron radiation applications. Their intrinsic resolving power $(\Delta E/E)$, although slightly dependent on the quality and surface preparation of the crystal, is better than 2000 at around 800 eV, and quite adequate for our application.

13.6p

FIG. 1. General layout of the RIPES apparatus.

Conventional BIS spectrometers usually operate, mainly for historical reasons, at the Al $K_\alpha$ emission energy (1486 eV),[16] and monochromatization is achieved by Bragg reflection on a spherically bent quartz $(10\bar{1}0)$ crystal in a Rowland circle mount (the so-called Johann geometry). Only one wavelength is diffracted and focused at the detector position, and the ultimate energy resolution is ~0.3–0.4 eV. This configuration is best suited for the collection of isochromat spectra, and it is also difficult to implement with beryl, which cannot easily be bent on a spherical surface. We have therefore abandoned the Rowland circle monochromator scheme, and adopted a solution based on a slitless spectrograph, coupled to a parallel detection system. The general layout of our apparatus, is schematically illustrated in Fig. 1. The focused, monochromatic electron beam excites a polychromatic source of x rays at the sample surface. The x rays are dispersed and sagittally focused onto a two-dimensional position-sensitive detector. The whole IPES spectrum is accumulated in parallel by performing a computer-controlled real-time position analysis of the signal from the detector.

### B. Optical design

The spectral analysis of the x-ray beam is performed by a crystal bent along a cylindrical surface. Figure 2 presents two schematic views of the Bragg spectrograph. The polychromatic photon source at the sample surface defines, with the centers of the crystal and of the detector, the horizontal scattering plane $\pi(x,y)$, which contains the cylinder axis **a**. The sample and detector are aligned along **a**, and the detector front surface lies in a vertical plane. This geometry, first described by von Hamos,[17] is particularly simple because the two optical functions, dispersion and focusing, are separate. The projection on the vertical plane $(xz)$ illustrates the focusing property of the cylindrically bent crystal. Assuming an infinitely narrow transmission function, a monochromatic point source is brought to a sharp focus on the axis, independent of the size of the crystal. For a polychromatic point source, different wavelengths are focused at different points along **a**. A point of the crystal surface closer to the source

15.6p

FIG. 2. Schematic view of the Bragg spectrograph (not to scale). *Top*: Vertical projection (focusing). *Bottom*: projection onto the horizontal scattering plane $\pi$ (dispersion).

will in fact define a larger Bragg angle than a more distant point ($\theta_1 > \theta_2$), and therefore a smaller diffracted energy. The photon energy dispersion relation along the axis is easily derived from the Bragg condition

$$E=(hc/2d)(1+Y^2/4R^2)^{1/2}, \quad (1)$$

where $R$ is the cylinder's radius and $Y$ is the distance between the source and the monochromatic image. In reality, both the transmission function and the source have a finite width, and the image acquires a finite dispersive width. This width is proportional to the convolution of the crystal rocking curve with the angular profile of the source, as seen from the detector. The cylinder radius $R$ is then determined by two conflicting requirements. $R$ should be small in order to maximize the total acceptance angle ($\sim 1/R^2$) and the total energy interval diffracted at a given crystal position ($\sim W/R$, where $W$ is the width of the crystal in the dispersive direction). At the same time, $R$ should be large enough to minimize the effect of a finite source size on the resolution. Also, the requirement that the sample and the crystal be located in different vacuum chambers sets a practical lower limit to $R$. A value $R=450$ mm was chosen as an acceptable compromise for our application.

We have used a simple ray-tracing program to estimate the optical properties and the expected energy resolution of the instrument. Figure 3 shows, for three different photon energies, and $R=450$ mm, the calculated images of a 10 mm line source perpendicular to the scattering plane. The $2d$ value was 15.95 Å (beryl) and the width of the crystal rocking curve was arbitrarily set to zero. Figure 3 shows the three corresponding images in a vertical plane, along a. The magnification is equal to 1, and the energy dispersion around 883 eV is ~0.4 eV/mm. A very slight curvature of the line images corresponds to an equivalent energy broadening of less than 40 meV. A totally negligible contribution is obtained for more realistic source length (~1 mm). Figure 3 also illustrates the influence of a finite crystal rocking curve and of a finite source width along the dispersive direction. A width of

20p

FIG. 3. *Top*: Diffracted image of a vertical line source from a cylindrical crystal ($R=450$ mm, $2d=15.95$ Å), for three different energies separated by 1 eV. The source width in the dispersive direction and the width of the crystal rocking curve have been arbitrarily set to zero; the vertical source size is 10 mm. The images lie in the detector plane. *Middle*: same as (top), but the source width in the dispersive direction is 1 mm, and the width of the rocking curve is 200 arcsec. *Bottom*: energy profiles obtained by summing the middle image along vertical lines.

1 mm, corresponding to ~180 arcsec, was added to the line source in the dispersive direction. The rocking curve had a Lorentzian shape with a full width at half-maximum (FWHM) of 200 arcsec, a conservative assumption for beryl at this energy.[18] The three images in the detector plane are still well separated. The FWHM of 0.55 meV can be taken as an estimate of spectrometer's contribution to the energy resolution.

### C. Description of the spectrometer

Our RIPES apparatus consists of three independent units: a sample chamber, containing the sample, the electron gun and some ancillary equipment; a crystal and a detector chamber. The axes of the three UHV chambers are perpendicular to a horizontal plate which represents the primary geometrical reference, and their relative positions coarsely define the Bragg angle. The sample chamber is directly mounted on the base plate, while the crystal and detector chambers can slide along precision bars in a direction parallel to a axis. By varying the relative position of the three chambers, it is possible to vary the Bragg angle $\Theta$ between 30° and 64° ($E\sim 865-1650$ eV, with a beryl crystal). The angular adjustment allowed by the coupling bellows is limited; large changes in the Bragg angle require breaking vacuum. This operation, however, does not interfere with the optical alignment of the spectrometer. The Bragg angle can be tuned over a limited range ($\Delta E\sim 25$ eV around 880 eV) by adjusting the positions of the crystal and of the detector within their chambers.This fine tuning is achieved by linear

motion feedthroughs driven by stepper motors, and it is routinely exploited in the normal mode of operation of the spectrometer, as will be discussed in the next section.

The sample is mounted at the end of a vertical He flow cryostat. An $xyz$ manipulator and a differentially pumped rotary feedthrough allow a fine adjustment of the sample position and a rotation around the vertical axis. The cryostat is equipped with a resistive heater and a Fe–Rh thermometer, and the sample temperature can be varied in a controlled way between 10 and 400 K. Clean surfaces of polycrystalline samples are usually prepared *in situ* by scraping with a diamond file, in a base pressure better than $1\times10^{-10}$ Torr. During normal operation, the sample and crystal chambers are separated by a leak-tight 1.5-$\mu$m-thick mylar window with a transmission of ~40% for photons of 880 eV.[19] The window has the double function of relaxing the vacuum requirements of the crystal and detector chambers (base pressure $2\times10^{-9}$ Torr), and of preventing scattered electrons generated by the $e$ gun from reaching the detector.

The electron gun is based on the compact design of Erdman and Zipf.[20] The indirectly heated BaO button cathode[21] is biased at the negative high voltage $-V_0$. The cathode is in close proximity with an extractor plate with a 1 mm circular aperture, followed by a three-element lens, and by a grounded output plate. The mean energy of the electron beam, with respect to the Fermi level of a grounded sample, is $E_K = eV_0 + \phi_{\text{cath}} + 2k_BT \sim eV_0 + 3$ eV, where $\phi_{\text{cath}}$ and $T$ are the cathode work function and temperature. After thermal activation of the BaO cathode, the gun can deliver a current of more than 1 mA at 880 V, but in normal measurement conditions the emission current is $I_{\text{cath}} = 0.2-0.3$ mA, with a thermal energy spread of ~0.2–0.3 eV. The measured sample current is approximately $0.5I_{\text{cath}}$. The beam diameter can be directly estimated from the visible fluorescence induced at the sample surface, or by measuring the image size at the detector. The minimum spot diameter, for a gun–sample distance of 3 cm, is ~5 mm when the focusing lens is operated as described in Ref. 20. However we have found that a sharp focus (~1 mm diam) can be obtained by reversing the lens polarity. This result has been confirmed by a computer simulation.[22] A focused beam is in general preferable, since the spot size defines the effective entrance slit of the spectrometer, but in particular circumstances the beam is defocused to reduce the current density at the sample. The effective dispersive source size can then be reduced, as customary, by choosing a more grazing emission angle. The electron gun can be retracted from the chamber and valved off to prevent unnecessary exposures to atmospheric pressure which would affect the subsequent performances of the cathode. We have observed cathode operating lifetimes in excess of three months at normal conditions.

The spectrograph is at present equipped with a $40\times25\times0.5$ mm$^3$ beryl $(10\bar{1}0)$ slab[23] glued onto a cylindrical substrate with a radius $R = 450$ mm. The slab is perfectly transparent and, at a visual inspection, free from inclusions and cracks. We have not measured the crystal rocking curve; however from previous experience with beryl crystals of similar quality installed on a monochromator for synchrotron radiation, and from published data,[18] we can estimate that the width of the rocking curve at 880 eV is of the order of, and probably better than, 200 arcsec. The solid angle accepted by the spectrograph is $\sim3.5\times10^{-3}$ s rad, and it is somewhat smaller than the acceptance angle of our conventional BIS spectrometer ($\sim5\times10^{-3}$ s rad).[16] The total energy interval diffracted around 880 eV by the 25-mm-wide slab is ~20 eV. A KAP (001) crystal, bent at the same radius, will later be used in RIPES measurements at the $N_5$ edge of uranium (736 eV). For this crystal the rocking curve width of 145 arcsec[24] at a Bragg angle of 39°, yields an expected intrinsic contribution of 0.6 eV, and a total resolution of 0.8 eV for a 1-mm-wide source. A rather wide photon energy range in the soft x-ray region could further be covered by the spectrometer by using readily available crystals like Si(111) (2200–4000 eV) or quartz $(10\bar{1}0)$ (1600–2900 eV).

The x-ray detection is performed by a commercial two-dimensional microchannel plate (MCP) detector equipped with a position analyzer.[25] The detector is a stack of three circular MCP's with a nominal active area diameter of 40 mm, followed by a resistive anode encoder (RAE). Photoelectrons generated at the front surface of the detector are multiplied by the MCPs, and collected by the RAE. The current pulses generated by each event at the four corners of the RAE are amplified and compared, to yield a pair of analog voltages proportional to the coordinates of the photon impact. These voltages are then converted by a fast ADC, and stored in a buffer. An additional MCP has been added to the standard two-MCP chevron stack, in order to increase the total gain, and consequently the spatial resolution, which is limited by the electronic noise in the RAE. The resulting resolution is, in both directions, better than 200 lines over the 40 mm of the whole detector, or 0.2 mm. Given a dispersion of 0.4 eV/mm at 880 eV, this value is much smaller than the expected total energy resolution of the spectrometer $\Delta E \sim 0.7$ eV (electrons plus photons). A CsI layer has been deposited on the front surface of the first MCP, in order to increase the detection efficiency in the spectral range of interest from 10% to approximately 25%. The dark noise of the detector is ~200 counts per minute (cpm) over the whole surface, or ~20 cpm within the electronically defined "active" window (see below). This figure corresponds to ~0.1 cpm per photon energy channel in the spectrum. During a real measurement, stray electrons, scattered x-rays, and possibly specularly reflected visible and UV photons, raise the noise level to ~0.5–1 cpm per channel, but these values remain small in comparison with the signal intensities of 10–100 cpm, that we have measured at resonance.

The spectrometer is controlled by a Macintosh IIVx computer, which is connected to various peripheral units (detector buffer, cathode voltage supply, stepper motors controller, sample temperature readout) via an IEEE interface. A dedicated program gives the possibility of choosing between three different acquisition modes. In the normal IPES mode, a full spectrum is collected at a fixed electron energy. The computer sets the required cathode voltage, calculates the new crystal and detector positions according to Eq. (1), and issues the appropriate commands to the stepper motors control unit. During the acquisition the program periodically polls the buffer. When a "buffer full" signal is detected, the

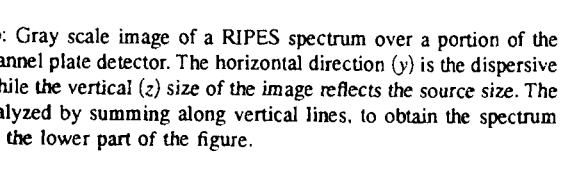

FIG. 4. Top: Gray scale image of a RIPES spectrum over a portion of the 2D microchannel plate detector. The horizontal direction ($y$) is the dispersive direction, while the vertical ($z$) size of the image reflects the source size. The image is analyzed by summing along vertical lines, to obtain the spectrum presented in the lower part of the figure.

coordinate pairs are downloaded into the computer, then converted to channel numbers ($0 \leq x,y \leq 199$), and summed to a $200 \times 200$ matrix, representing a two-dimensional (2D) image of the detector. Figure 4 (top) shows a 10-mm-high portion of such an image along the equatorial plane of the detector. The horizontal direction is the dispersive direction, and the vertical size reflects the nondispersive source size. The IPES spectrum of Fig. 4 (bottom) is obtained, as in Fig. 3, by a sum along vertical lines, within limits chosen to include the whole signal, and to reject the noise from further pixels. This solution is more flexible than a solution based on a simpler one-dimensional detector, since the large nondispersive size allows one to compensate electronically for possible alignment errors in the spectrometer. The two other possible acquisition modes, the constant final state (CFS) and the constant photon energy (CPE) modes, are described, with examples, in Sec. IV.

## IV. SYSTEM PERFORMANCES

### A. Preliminary results

We have performed some preliminary IPES measurements of samples that do not present a resonance behavior in the spectral domain of interest. As an example, Fig. 5 shows the IPES spectrum of polycrystalline cobalt measured at an primary energy of 880 eV. The spectrum shows a prominent feature near the Fermi level, which reflects the unoccupied part of the Co $3d$ band, in agreement with BIS data collected at 1486 eV.[26] The measured intensity on the peak was ~1 count per minute (cpm) per channel and the total acquisition time (6 h) of the same order of magnitude as the accumulation time for a conventional BIS spectrum. We have observed larger intensities, of the order of 2–3 cpm, on the empty $4f$ peak of polycrystalline lanthanum.

By tracking, for a constant excitation energy, the position of the spectral features as the detector was displaced in a controlled way along the dispersive direction, we have measured the actual width of the active region (37.5 mm). By



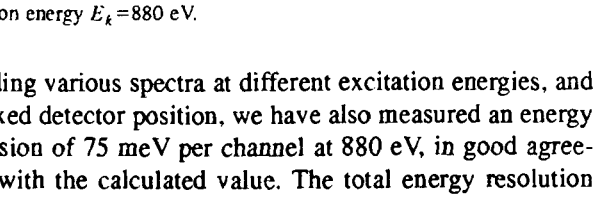

FIG. 5. IPES spectrum of a polycrystalline cobalt sample, measured at an excitation energy $E_k = 880$ eV.

recording various spectra at different excitation energies, and at a fixed detector position, we have also measured an energy dispersion of 75 meV per channel at 880 eV, in good agreement with the calculated value. The total energy resolution $\Delta E$ of the spectrometer can be estimated from the spectrum of Fig. 5. The 10%–90% width of its leading edge, ~0.8 eV, is as an upper limit to $\Delta E$, since the electronic density of states varies rapidly around $E_F$, and the spectral line shape cannot be interpreted as a simple metallic edge.[26] Spectra of copper, which is characterized by a flat $s$ band, yield $\Delta E \sim 0.6$–$0.7$ eV for an electron current of 0.3 mA; the large uncertainty reflecting the low intensity (<0.5 cpm) and poor signal to noise ratio. Measurements at resonance require much shorter accumulation times, so that possible long-term drifts of the electron energy and of the detector electronics are negligible; moreover they are carried out at a lower electron current, and therefore at a lower cathode temperature. We then estimate that the instrument can attain a resolution of ~0.6 eV.

We have also measured the uniformity of the gain across the detector by recording spectra at various detector positions, and constant electron energy. We have observed smooth variations of a few percent over most of the detector surface, and slightly larger changes near the edge. In an analogous way we have looked for inhomogeneities of the crystal reflectivity, by scanning the crystal position. These results have been later confirmed with higher accuracy by resonant spectra of Ce materials, where the intensity is considerably larger. This uniformity is sufficient in most circumstances. However, to prevent any spurious modulation of the spectra across the resonance, the crystal and the detector positions are adjusted for each electron energy, so that a given structure in the spectrum (i.e., a structure at a fixed energy with respect to the Fermi level) is tied to the same position on the crystal and on the detector.

### B. RIPES of cerium systems

Figure 6 illustrates typical performances of the apparatus in the RIPES mode, near the Ce $M_5$ absorption edge. A series of spectra of the intermetallic compound $CeNi_2$, have been measured at increasing excitation energies, from 878 eV (below resonance) to 888 eV (above resonance), in 1 eV

FIG. 6. IPES spectra of $CeNi_2$ measured at increasing excitations energies from below to above the Ce $M_5$ absorption edge. The horizontal shifts of the curves reflect the corresponding increase of the electron energy. The horizontal bars indicate the typical sizes and positions of the "$f^1$" and "$f^2$" windows in a constant final state measurement.

steps.[27] The measurements have been performed, as described above, by adjusting the crystal and detector positions for each excitation energy. The spectra therefore always appear at the same position on the detector, while the photon energy corresponding to its leading edge increases by 1 eV for each curve. The horizontal shifts of the curves correspond to the 1 eV steps of the excitation energy. As expected, a rapid evolution of the spectra is observed near the edge. The overall intensity, which below threshold is comparable to that of conventional BIS, increases by approximately 2 orders of magnitude in a narrow interval around $E_k$=883 eV. In these conditions a RIPES spectrum can be collected in a few minutes, compared to the several hours of a conventional BIS spectrum.

The spectral line shape is strongly energy dependent. Two different structures can be identified in the spectrum, near $E_F$ and around 5 eV. They correspond, within the Anderson model, to final states with $4f^1$ and $4f^2$ character. If the intensity under the two peaks is recorded as a function of electron energy, two distinct resonances can be readily identified. In this CFS mode of acquisition, the electron kinetic energy is increased in steps. At each step the crystal and detector positions are adjusted as for a normal spectrum, and the integrated signals within two selected photon energy windows are recorded. Fig. 7 shows two such curves for a sample of $\alpha$-Ce, the low temperature phase of cerium, prepared by evaporating a thin layer of Ce onto a cold (10 K) Cu substrate. The two resonances, schematically labeled as $4f^0+e\rightarrow c4f^2\rightarrow 4f^1+h\nu$, and $4f^1+e\rightarrow c4f^3\rightarrow 4f^2+h\nu$, are sharp and well separated in energy. Their relative strength reflects the relative weight of the $4f^0$ and $4f^1$ configurations in the initial state. We have observed large variations of this ratio in different Ce-based systems, in strong correlation with the characteristics Kondo temperatures.

Figure 7 also shows a CPE curve, obtained by scanning the electron kinetic energy, and integrating the signal within a constant window at a *fixed* photon energy. The window had the same width as the "$f^1$" CFS window, and it was centered around the photon energy of the characteristic Ce $M_\alpha$ emission. The Ce $M_\alpha$ emission which can be described by the transition $4f^1+e\rightarrow c4f^2k\rightarrow 4f^1+h\nu^*$, where $k$ is a conduction electron, is indistinguishable from the RIPES process at resonance. It occurs at constant photon energy and is therefore analogous to an Auger line in photoemission. Above threshold, the CPE curve reflects the incoherent superposition of the Ce $M_\alpha$ emission and of the IPES spectrum that "drifts" through the sampling window as the excitation energy is increased. Well above threshold its intensity is fairly insensitive to the small variations of the $4f$ occupancy in different materials, and therefore provides an interesting internal calibration for the CFS curves.

FIG. 7. CFS curves for the $f^1$ and $f^2$ spectral features from a sample of $\alpha$-Ce, prepared and measured at 10 K. The dotted line is a constant photon energy curve, measured at a photon energy equal to that of the Ce $M_\alpha$ characteristic emission.

## V. DISCUSSION

In this paper we have described the motivations, the design considerations, and some preliminary results of a new UHV spectrometer for resonant inverse photoemission. The instrument has demonstrated the predicted performances and is now routinely operated in our laboratory. Our data on cerium compounds confirm the considerable advantages of RIPES over conventional BIS. The nature of the resonance process brings about a substantial reduction of the acquisition time, and the possibility of tuning the relative sensitivity to the Ce $4f$ and the conduction band states, by almost three orders of magnitude, by a change of just a few eV's in the excitation energy.[28] We are exploiting these features to perform previously infeasible time- or temperature-dependent experiments on a single surface, and studies of thin (submonolayer) Ce overlayers. We also anticipate stimulating future developments when we explore the resonant behavior of other correlated materials like high-$T_c$ cuprates and uranium-based materials.

## ACKNOWLEDGMENTS

This work has been supported by the Swiss National Science Foundation. We thank Dr. B. Dardel for his help with the development of the acquisition program, and gratefully acknowledge the expert technical assistance of F. Chatelain and D. Varidel.

[1] W. Duane and F. L. Hunt, Phys. Rev. **6**, 166 (1915).
[2] B. R. A. Nijboer, Physica **12**, 461 (1946).
[3] J. B. Pendry, Phys. Rev. Lett. **45**, 1356 (1980).
[4] For a recent review, and a discussion of the implications of this statement, see: *Unoccupied Electronic States* edited by J. C. Fuggle and J. E. Inglesfield (Springer, Berlin, 1992).
[5] J. Zaanen and G. A. Sawatzky, Can. J. Phys. **65**, 1262 (1987).
[6] J. K. Lang, Y. Baer, and P. A. Cox, J. Phys. F **11**, 121 (1981).
[7] J. W. Allen, S. J. Oh, O. Gunnarsson, K. Schönhammer, M. B. Maple, M.S. Torikachvili, and I. Lindau, Adv. Phys. **35**, 275 (1986).
[8] U. Fano, Phys. Rev. **124**, 1866 (1961).
[9] L. C. Davis, J. Appl. Phys. **59**, R25 (1986).
[10] R. J. Liefeld, A. F. Burr, and M. B. Chamberlain, Phys. Rev. A **9**, 316 (1974); M. B. Chamberlain, A. F. Burr, and R. J. Liefeld, *ibid.* **9**, 663 (1974).
[11] F. Riehle, Ph.D. thesis, Karlsruhe, 1977; Jpn. J. Appl. Phys. **17**, Suppl. 17-2, 314 (1978).
[12] F. Riehle, Phys. Status Solidi **98**, 245 (1980).
[13] A. S. Shulakov, T. M. Zimkina, and V. A. Formichev, Izv. AN SSSR **49**, 1495 (1985).
[14] H. Petersen and H. Baumgärtel, Nucl. Instrum. Methods **172**, 191 (1980).
[15] J. Nordgren, G. Bray, S. Cramm, R. Nyholm, J.-E. Rubensson, and N. Wassdahl, Rev. Sci. Instrum **60**, 1690 (1989).
[16] J. K. Lang and Y. Baer, Rev. Sci. Instrum. **50**, 221 (1979).
[17] L. von Hamos, Z. Kristallogr. **101**, 17 (1939).
[18] Z. Hussain, E. Umbach, D. A. Shirley, J. Stöhr, and J. Feldhaus, Nucl. Instrum. Methods **195**, 115 (1982).
[19] B. L. Henke and P. A. Jaanimagi, Rev. Sci. Instrum. **56**, 1537 (1985).
[20] P. W. Erdman and E. C. Zipf, Rev. Sci. Instrum. **53**, 225 (1982).
[21] Number 3322.143.94605, Philips AG, Zürich.
[22] K. Fauth (private communication).
[23] Quartz & Silice, Nemours, France.
[24] B. L. Henke, P. Lee, T. J. Tanaka, R. L. Shimabukuro, and B. K. Fujikawa, At. Data Nucl. Data Tables **27**, 1 (1982).
[25] Model 3300/2401, Quantar Technology Inc., Santa Cruz, CA.
[26] W. Speier, J. C. Fuggle, R. Zeller, B. Ackermann, K. Szot, F. U. Hillebrecht, and M. Campagna, Phys. Rev. B **30**, 6921 (1984).
[27] P. Weibel, M. Grioni, D. Malterre, B. Dardel, and Y. Baer, Phys. Rev. Lett. **72**, 1252 (1994).
[28] P. Weibel, M. Grioni, D. Malterre, O. Manzardo, Y. Baer, and G. Olcese (to be published).

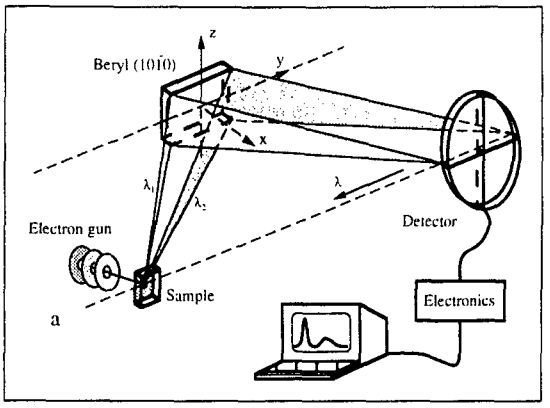


Fig. 1

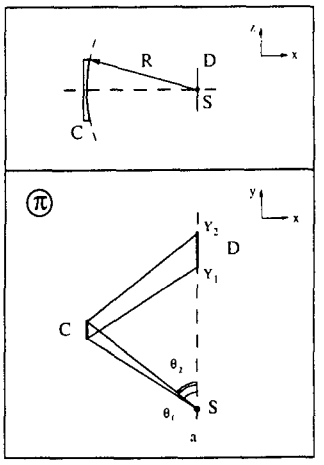


Fig. 2

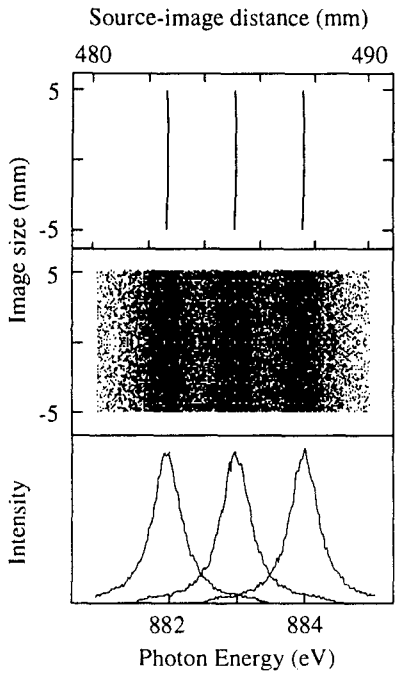


Fig. 3

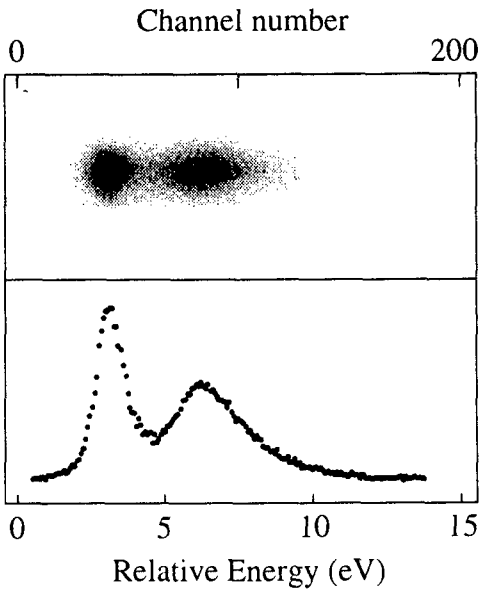


Fig. 4

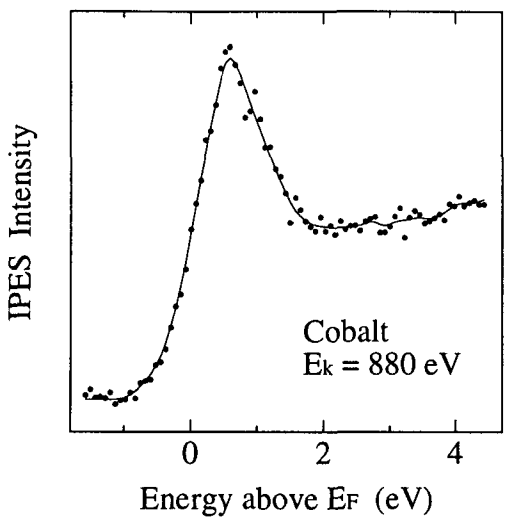


Fig. 5

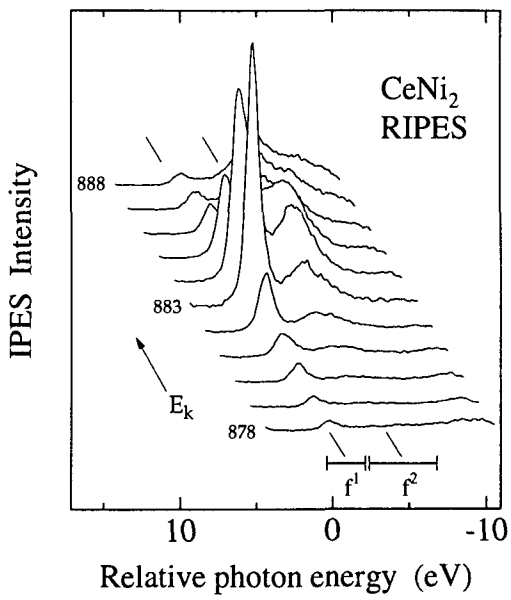


Fig. 6

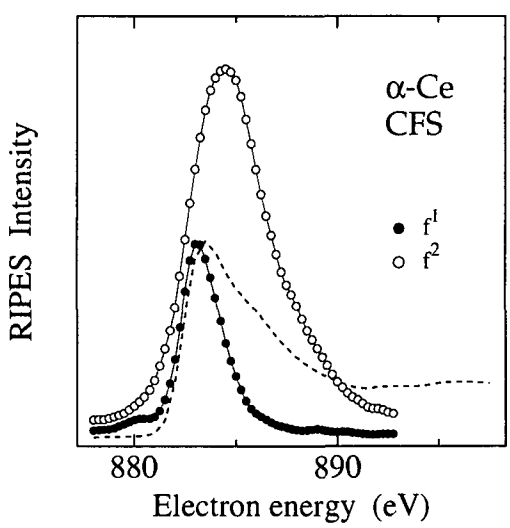


Fig. 7

# Resonant Inverse Photoemission: A New Probe of Correlated Systems

P. Weibel, M. Grioni, D. Malterre, B. Dardel, and Y. Baer
*Institut de Physique, Université de Neuchâtel, CH-2000 Neuchâtel, Switzerland*
(Received 20 September 1993)

Inverse photoemission measurements of cerium compounds reveal a strong energy dependence near the Ce $M_5$ ($3d_{5/2} \rightarrow 4f$) absorption edge. Two separate resonances, resulting from configuration mixing in the ground state, are identified for the first time. Their relative intensities reflect the different hybridization strengths in various Ce-based materials. Because of its site and symmetry selectivity, resonant inverse photoemission is potentially a valuable technqiue for the investigation of correlated materials, complementary to the well-established resonant photoemission spectroscopy.

PACS numbers: 71.28.+d, 78.70.En, 79.20.Hx

High-energy spectroscopies play a prominent role in the investigation of valence fluctuation in cerium compounds [1-7]. They have contributed to identifying the partially localized character of the strongly correlated Ce $4f$ electrons and to establishing a description of these electronic states based on the degenerate Anderson impurity model [8-10]. Photoemission (PES) and inverse photoemission (IPES) spectroscopy can in principle be interpreted as the many-body spectral function derived from the Anderson Hamiltonian. A reliable analysis of the experimental results, however, depends on the ability to separate the $4f$ contribution from that of other electronic states. In PES, this crucial problem is usually tackled by comparing spectra at various excitation energies, to take advantage of the different energy dependence of the photoionization cross section for the $4f$ and the band states. Unfortunately, in many Ce systems an unambiguous determination of the $4f$ spectral weight is hindered by a large band contribution [11]. The development of resonant PES (RESPES), which exploits the occurrence of resonances in the $4f$ cross section when the photon energy is tuned to an appropriate absorption edge, has provided a clear breakthrough in this field. Because of the localized nature of the core hole, and to the dipole selection rules, RESPES spectra obtained at the Ce $N_{4,5}$ $(4d)^4$ and $M_{4,5}$ $(3d)$ edge [12] essentially reflect the $4f$ contribution at the Ce site, and have recently been interpreted within the framework of the Anderson model [13].

Conventional inverse photoemission measurements are traditionally performed either in the vacuum ultraviolet (VUV) range ($5 < h\nu < 30$ eV) or at the Al $K_\alpha$ characteristic energy (1486.6 eV). IPES spectra of Ce compounds measured at the lower end of the VUV range are dominated by emission from band states. In the x-ray region the $4f$ signal is clearly visible, but the subtraction of the non-$f$ and inelastic background is not always straightforward. Moreover, the IPES cross section is by orders of magnitude smaller than the corresponding PES cross section [14], which imposes long measuring times and rules out the investigation of interesting samples like diluted materials or adsorbates. It would be highly desirable to improve this situation by exploiting resonances of the IPES cross section.

The existence of a resonant enhancement of the bremsstrahlung emission was first demonstrated by the pioneering work of Liefeld, Burr, and Chamberlain [15] and Riehle [16] on metallic La and Ce. Resonances were later observed also in Ni and Sc in the x-ray [17] and VUV [18] range. The early results [15,16], however, as well as subsequent theoretical [19] and experimental [20] work, were mainly concerned with the case of $f^0$ La, and spectra of metallic Ce were interpreted with the assumption of integer valence. This conceptual limitation, as well as the technical difficulties of the experiment, prevented resonant IPES from ever being considered as a spectroscopic probe of valence fluctuators. In every respect the situation is different today. In the last decade important advances have been made in the understanding of the ground state and spectral properties of Ce materials. Significant improvements, fostered by the development of synchrotron radiation beam lines, have also been achieved in the monochromatization and detection of soft x rays. In this Letter we demonstrate the potentialities of resonant IPES (RIPES) which now appears as a promising new tool for investigating the electronic properties of Ce compounds, on the same footing as RESPES.

The RIPES measurements were performed near the Ce $M_5$ absorption edge (883 eV) in a dedicated IPES spectrometer. Electrons were generated by an electron gun equipped with an indirectly heated BaO cathode. The kinetic energy of the electrons $E_K \sim V_c + \Phi$, where $\Phi \sim 2.5$ eV is the work function of the BaO cathode, could be varied continuously by adjusting the cathode voltage. The width of the electron distribution was 0.3-0.5 eV. The emitted photons were dispersed by a Bragg reflection on a beryl $(10\bar{1}0)$ crystal onto a microchannel plate detector equipped with a resistive anode encoder. The theoretical energy resolution of the spectrograph, determined by the crystal's rocking curve, is approximately 0.4 eV at the Ce $M_5$ edge. The actual resolution is determined by the size of the illuminated area on the sample, which acts as the entrance slit of the monochromator. Experiments were carried out with a total energy resolution (electrons plus photons) of ~0.6-0.8 eV. Poly-


0031-9007/94/72(8)/1252(4)$06.00

crystalline samples prepared in an arc furnace were cleaned *in situ* by scraping with a diamond file at a base pressure of $1\times10^{-10}$ torr, and measured at room temperature.

Within the framework of the Anderson model the $4f$ IPES spectral function of a Ce impurity is predicted to exhibit peculiar features that reflect the hybrid character of the singlet ground state. In the limit of large Coulomb repulsion the ground state has, in simplified notation, the form $|\Psi_G\rangle = a|f^0\rangle + b|f^1\rangle$, where $f^0$ and $f^1$ indicate configurations of the Ce impurity with zero and, respectively, one $4f$ electron. The addition of one $4f$ electron in an IPES experiment couples the $f^0$ and $f^1$ configurations of the ($N$-electron) ground state $|\Psi_G\rangle$ to the $f^1$ and $f^2$ character of ($N+1$)-electron final states. Symbolically we indicate these transitions as $|f^0\rangle + e^- \rightarrow |f^1\rangle + h\nu$, and $|f^1\rangle + e^- \rightarrow |f^2\rangle + h\nu$. The former generate a sharp peak near the Fermi level (the "Kondo peak"), with spin-orbit and crystal field satellites. The latter yield a structure, broadened by multiplet effects, 4–5 eV above $E_F$. Because of the limited experimental energy resolution of IPES, the Kondo peak and its satellites cannot be resolved, and appear as a single peak. The intensity of this peak is proportional to the weight of the $f^0$ configuration in the ground state, and is therefore a sensitive indicator of hybridization. In addition to this normal IPES process, when the excitation energy reaches the $3d$ absorption edge of Ce, new transitions from $|\Psi_G\rangle$ that involve the creation of a $3d$ core hole ($\underline{c}$) become possible:

$$|f^0\rangle + e^- \rightarrow |\underline{c}f^2\rangle \rightarrow |f^1\rangle + h\nu, \quad (1)$$

$$|f^1\rangle + e^- \rightarrow |\underline{c}f^3\rangle \rightarrow |f^2\rangle + h\nu. \quad (2)$$

Since these transitions have the same initial state ($|\Psi_G\rangle$) and the same final states as the normal IPES transitions, quantum interference with the direct processes must produce resonances in the transition rates [21]. A strong enhancement of the whole spectrum can therefore be anticipated at the edge energy.

In order to test this prediction, we have performed an energy dependent investigation of $CeNi_2$, a compound characterized by a rather strongly hybridized ground state, with an estimated Kondo temperature $T_K \sim 900$ K [4]. Figure 1 shows a set of IPES spectra of $CeNi_2$, collected around the Ce $M_5$ edge, and labeled by the accelerating cathode voltage $V_c$. At the lowest excitation energy ($V_c = 874$ eV) the signal level was comparable to that of conventional IPES spectra obtained at 1486 eV in our laboratory. Spectral features, however, can be barely distinguished on the scale of Fig. 1. Increasing the electron energy has two clear effects on the IPES spectra: a corresponding shift to higher photon energy, and a dramatic resonant enhancement of 2 orders of magnitude around 880 V.

The comparison, in Fig. 2, of the 880 and 882 V spectra, shows that the IPES spectral intensity is not uniformly enhanced at resonance. The 880 V spectrum is dominated by the $f^1$ peak near $E_F$, and the $f^1/f^2$ ratio is considerably larger than in a conventional IPES spectrum (inset). The ratio between the $4f$ signal and the non-$f$ and inelastic background ($B$) is also strongly increased, demonstrating the sensitivity of RIPES to the $4f$ states. The separation between the $f^1$ peak and the center of the $f^2$ structure is smaller than in the IPES spectrum at 1486 eV, and it increases between 880 and 882 V. At 882 V the $f^1$ signal is reduced to about 30% of its resonance value, and the $f^2$ intensity has roughly doubled. Between the $f^1$ and $f^2$ peaks in the 882 V spectrum, we observe the characteristic Ce $M_\alpha$ line that corresponds to the transitions

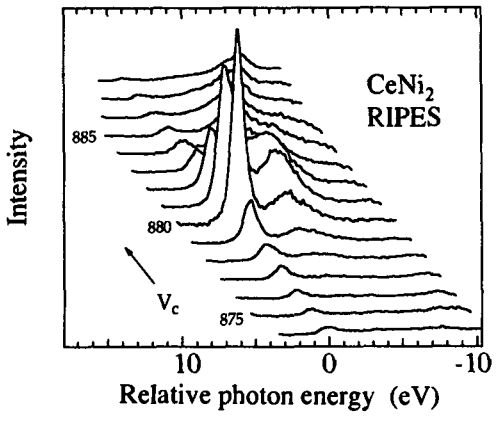


FIG. 1. Inverse photoemission spectra of $CeNi_2$ collected at various excitation energies through the Ce $M_5$ ($3d_{5/2}$) absorption edge. The spectra are labeled by the accelerating voltage of the primary electron beam. The photon energy zero was arbitrarily set.

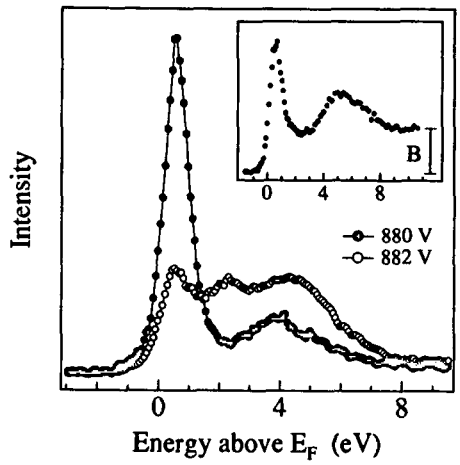


FIG. 2. RIPES spectra of $CeNi_2$ from Fig. 1, corresponding to the maximum of the $f^1$ (880 V) and $f^2$ (882 V) emission. At variance with Fig. 1, the spectra have been shifted with respect to each other to compensate for the different primary energy. The intermediate feature visible at 882 V is the characteristic Ce $M_\alpha$ line. Inset: Conventional IPES spectrum ($h\nu = 1486$ eV) of $CeNi_2$.

$$|f^1\rangle + e^- \rightarrow |\underline{c}f^2 k\rangle \rightarrow |f^1 k\rangle + h\nu^*, \quad (3)$$

where $k$ represents a conduction band electron. The $M_\alpha$ line is degenerate with the $f^1$ peak at threshold and drifts away from the $f^1$ peak with increasing excitation energy. This behavior is therefore analogous to that of characteristic Auger emissions in resonant PES.

We have separately measured the primary energy dependence of the $f^1$ and $f^2$ peaks by integrating the IPES signal within two windows (respectively, 2.5 and 5 eV wide) that tracked the position (i.e., the photon energy) of the two peaks on the detector. The resulting constant final state curves (CFS) of Fig. 3 demonstrate that the two spectral features resonate at distinct energies, separated by $\sim 2$ eV. This value is in very good agreement with our simple model that predicts a separation $\Delta E = E(\underline{c}f^3) - E(\underline{c}f^2) \sim \varepsilon_f + 2U_{ff} + U_{fc} \sim 2$ eV, where $E(\underline{c}f^3)$ and $E(\underline{c}f^2)$ represent the energies of the two intermediate-state configurations, and where we have used typical values for the $4f$ energy $\varepsilon_f$ ($-2$ eV), the $f$-$f$ Coulomb repulsion $U_{ff}$ (7 eV), and the core hole-$4f$ Coulomb interaction $U_{fc}$ ($-10$ eV).

A quantitative analysis of the resonance profiles would require an elaborate treatment of the RIPES process, which takes into account the multiplet structure, hybridization, and coupling of the relevant configurations. Such a calculation is clearly beyond the scope of this Letter. We just remark that the widths of both the $f^1$ (2 eV) and the $f^2$ (4 eV) CFS curves are considerably narrower than the $\underline{c}f^2$ and $\underline{c}f^3$ manifolds, that extend over many eV's. We interpret this sharpening as a consequence of selection rules that limit, in the excitation [22] and especially in the deexcitation [23] processes, the number of allowed transitions.

The high sensitivity of RIPES to the nature of the ground state is illustrated by the comparison of different Ce materials. The $4f$ electrons are weakly hybridized in CeSb, which orders below 16 K with a magnetic moment close to that of a free $Ce^{3+}$ ion [24]. Core level PES results [3], as well as conventional IPES [25] and high-resolution PES, also indicate a very small hybridization. The CFS curves of Fig. 3 demonstrate a striking difference with respect to $CeNi_2$, since the $f^2$ peak dominates a very weak "$f^1$" structure. Minor differences concern the smaller separation of the two maxima and the width of the $f^2$ CFS (3.25 eV). The vanishingly small intensity in the $f^0 \rightarrow f^1$ channel is consistent with an almost pure $f^1$ ground state configuration. We believe that the weak "$f^1$" feature essentially reflects the $M_\alpha$ emission (3), whose intensity is not related to the weight of the $f^0$ configuration. Since the $M_\alpha$ emission yield is not expected to be very different in $CeNi_2$ and CeSb, its small intensity in CeSb justifies the decision to neglect it also in $CeNi_2$. The variation of the $f^1/f^2$ intensity ratio observed between $CeNi_2$ and CeSb, and in preliminary measurements of other cerium compounds characterized by intermediate values of $T_K$, demonstrates that the intensity of the sharp $f^1$ resonance is a sensitive measure of configuration mixing in the initial state. The early measurements of $\gamma$-Ce of Ref. [15] also appear to follow this trend, although the occurrence of an $f^0 \rightarrow f^1$ resonance was not recognized at that time. The presence of a double resonance appears as a novel and general feature of the electron-addition spectral function of Ce materials. The material-dependent shape of the resonance reflects the configuration mixing in the ground state and sets independent constraints on the parameters of the Anderson Hamiltonian. Its description should therefore be considered as an important challenge for future theoretical work.

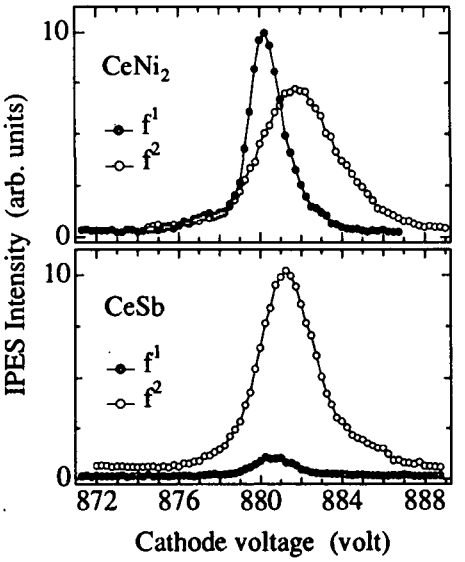


FIG. 3. Constant final state (CFS) curves for $CeNi_2$ (top) and CeSb (bottom). The curves are obtained by integrating, as a function of excitation energy, the RIPES signal within two energy windows (respectively 2.5 and 5 eV wide) that follow the position of the $f^1$ and the $f^2$ peaks.

In conclusion, we have demonstrated in this Letter that the resonance occurring at the Ce $3d$ edge amplifies by roughly 2 orders of magnitude the conventional $4f$ bremsstrahlung cross section, so that this technique opens unprecedented possibilities to study valence fluctuations in Ce compounds. Resonant IPES offers for the investigation of the unoccupied states the same advantages as resonant PES for the occupied states. The site and symmetry selectivity is of crucial importance in many problems. Moreover, a number of investigations that are at present problematic or even impossible because of the inherently low signal level of IPES will become accessible with RIPES. Typical examples are detailed temperature-dependent studies of Ce materials [26], as well as surface or cluster studies, or even the use of dichroism. In perspective, we anticipate that RIPES will allow important progress in the investigation of the empty states in other correlated systems, like the uranium compounds. From the theoretical side, we hope that the present

demonstration of the power of this technique will motivate, beyond existing models [19,27], reliable calculations of the resonance profiles and of the energy-dependent spectral line shape, which are obvious prerequisites for the quantitative exploitation of this technique.

This work has been supported by the Fonds National Suisse de la Recherche Scientifique. We thank G. Schmerber who prepared and characterized the CeSb sample. One of us (M.G.) acknowledges stimulating discussions with G. van der Laan.

[1] J. M. Lawrence, P. S. Riseborough, and R. D. Parks, Rep. Prog. Phys. **44**, 1 (1981).
[2] P. A. Lee, T. M. Rice, J. W. Serene, L. J. Sham, and J. W. Wilkins, Comments Condens. Matter Phys. **12**, 99 (1986).
[3] J. C. Fuggle, F. U. Hillebrecht, Z. Zolnierek, R. Lässer, Ch. Freiburg, O. Gunnarsson, and K. Schönhammer, Phys. Rev. B **27**, 7330 (1983).
[4] J. W. Allen, S. J. Oh, O. Gunnarsson, K. Schönhammer, M. B. Maple, M. S. Torikachvili, and I. Lindau, Adv. Phys. **35**, 275 (1986).
[5] Y. Baer and W. Schneider, in *Handbook on the Physics and Chemistry of Rare-Earths*, edited by K. A. Gschneider, Jr., L. Eyring, and S. Hüfner (North-Holland, Amsterdam, 1987), Vol. 10, p. 1.
[6] A. Kotani, T. Jo, and J. C. Parlebas, Adv. Phys. **37**, 37 (1988).
[7] F. Patthey, J. M. Imer, W.-D. Schneider, H. Beck, and Y. Baer, and B. Delley, Phys. Rev. B **42**, 8864 (1990).
[8] O. Gunnarsson and K. Schönhammer, Phys. Rev. B **28**, 4315 (1983).
[9] P. Coleman, Phys. Rev. B **29**, 3035 (1984).
[10] N. E. Bickers, D. L. Cox, and J. W. Wilkins, Phys. Rev. Lett. **54**, 230 (1985); Phys. Rev. B **36**, 2036 (1987).
[11] D. Malterre, M. Grioni, P. Weibel, B. Dardel, and Y. Baer, Phys. Rev. B **48**, 10599 (1993).
[12] C. Laubschat, E. Weschke, C. Holtz, M. Domke, O. Strebel, and G. Kaindl, Phys. Rev. Lett. **65**, 1639 (1990); E. Weschke, C. Laubschat, T. Simmons, M. Domke, O. Strebel, and G. Kaindl, Phys. Rev. B **44**, 8304 (1991).
[13] O. Gunnarsson and T. C. Li, Phys. Rev. B **36**, 9488 (1987); O. Gunnarsson and K. Schönhammer, in *Giant Resonances in Atoms, Molecules, and Solids*, edited by J. P. Connerade, J.-M. Esteva, and R. C. Karnatak (Plenum, New York, 1987), p. 405.
[14] J. B. Pendry, Phys. Rev. Lett. **45**, 1356 (1980).
[15] R. J. Liefeld, A. F. Burr, and M. B. Chamberlain, Phys. Rev. A **9**, 316 (1974); M. B. Chamberlain, A. F. Burr, and R. J. Liefeld, Phys. Rev. A **9**, 663 (1974).
[16] F. Riehle, Ph.D. thesis, Karlsruhe, 1977 (unpublished); Jpn. J. Appl. Phys. **17**, Suppl. 17-2, 314 (1978).
[17] F. Riehle, Phys. Status Solidi B **98**, 245 (1980).
[18] Y. Hu, T. J. Wagener, Y. Gao, and J. H. Weaver, Phys. Rev. B **38**, 12708 (1988).
[19] G. Wendin and K. Nuroh, Phys. Rev. Lett. **39**, 48 (1977); K. Nuroh and G. Wendin, Phys. Rev. B **24**, 5533 (1981).
[20] P. Motais, E. Belin, and C. Bonnelle, Phys. Rev. B **30**, 4399 (1984).
[21] U. Fano, Phys. Rev. **124**, 1866 (1961).
[22] V. O. Koustroun, M. H. Chen, and B. Crasemann, Phys. Rev. A **3**, 533 (1971).
[23] B. T. Thole, G. van der Laan, J. C. Fuggle, G. A. Sawatzky, R. C. Karnatak, and J.-M. Esteva, Phys. Rev. B **32**, 5107 (1985).
[24] J. X. Boucherle, A. Delapalme, C. J. Howard, J. Rossat-Mignod, and O. Vogt, Physica (Amsterdam) **102B**, 253 (1980).
[25] F. U. Hillebrecht, W. Gudat, N. Mårtensson, D. D. Sarma, and M. Campagna, J. Magn. Magn. Mater. **47&48**, 221 (1985).
[26] D. Malterre, M. Grioni, P. Weibel, B. Dardel, and Y. Baer, Phys. Rev. Lett. **68**, 2656 (1992); Europhys. Lett. **20**, 445 (1992).
[27] S. Tanaka, Y. Kayanuma, and A. Kotani, J. Phys. (Paris) Colloq. **8**, 735 (1988); J. Phys. Soc. Jpn. **59**, 1488 (1990).

EUROPHYSICS LETTERS 10 March 1995

*Europhys. Lett.*, **29** (8), pp. 629-634 (1995)

# Resonance and Anti-Resonance in Inverse Photoemission: Discriminating Localized and Extended States in Cerium Systems.

P. WEIBEL (*), M. GRIONI (*), D. MALTERRE (*) (§), O. MANZARDO (*)
Y. BAER (*) and G. L. OLCESE (**)

(*) *Institut de Physique, Université de Neuchâtel - CH-2000 Neuchâtel, Switzerland*
(**) *Istituto di Chimica Fisica dell'Università - Corso Europa, Genova, Italy*

(received 13 December 1994; accepted 16 February 1995)

PACS. 71.28+d – Narrow-band systems; heavy-fermion solids; intermediate-valence solids.
PACS. 78.70En – X-ray emission threshold and fluorescence.
PACS. 79.20Hx – Electron impact: secondary emission.

**Abstract.** – The electron addition spectrum of the intermediate-valence material $CeRh_3$ exhibits a dramatic dependence on the excitation energy near the Ce $M_5$ ($3d \rightarrow 4f$) absorption edge. The cerium $4f$ spectral intensity is first strongly depressed, and then resonantly enhanced with respect to the band contribution, with an overall cross-section variation of almost three orders of magnitude. These results show that, in close analogy with resonant photoemission, a comparison of on- and off-resonance spectra can be used to identify and separate the signal from the localized and the extended electronic states in Ce systems.

Resonances are well-known phenomena in atomic and solid-state physics [1,2]. Besides being the object of active fundamental research, they offer unique opportunities for the investigation of the electronic structure of materials. The development of resonant photoemission (RESPES) has led in particular to considerable advances in the study of cerium-based valence fluctuators [3]. These materials exhibit peculiar physical properties associated with the partially localized Ce $4f$ electrons, and are usually described within the framework of the Anderson impurity model (AIM). High-energy spectroscopies, and namely photoemission (PES, electron removal) and inverse photoemission (IPES, electron addition) can provide a stringent test of the spectral properties of the model, and verify the predicted scaling behaviours [4-8]. The combined PES/IPES spectral function of Ce materials is in fact expected to display all the relevant energy scales of the Anderson Hamiltonian, from the large energy scales reflecting charge fluctuations, to the emerging Kondo scale, characteristic of spin fluctuations. The site and atomic symmetry selectivity of RESPES is often exploited to greatly enhance the sensitivity to the $4f$ states with respect to different orbital symmetries. Most of the RESPES work has been carried out at the $4d \rightarrow 4f$ giant resonance

(§) Present address: Laboratoire de Physique du Solide, Université de Nancy, BP 239, Vandoeuvre les Nancy, France.

of cerium ($N_{4,5}$ edge ~ 120 eV), but sporadic measurements have been performed near the $3d \rightarrow 4f$ thresholds of some rare earths [9, 10], and also of Ce ($M_{4,5}$ edge ~ 883 eV) [11, 12].

Inverse photoemission plays a unique role in the spectroscopy of Ce systems. It is in fact directly sensitive to the distinctive spectral feature of these materials, the Kondo resonance, which is mostly unoccupied and therefore largely inaccessible to PES. Unfortunately conventional IPES measurements, performed for technical reasons at a fixed photon energy of 1486 eV, often suffer from severe limitations due to a weak signal. Previous results demonstrated the existence of a resonance of the IPES cross-section near the $M_{4,5}$ [13, 14] and the $N_{4,5}$ [15] edges, but this attractive opportunity was never exploited. Recently we have shown that the strong intensity amplification at the Ce $M_5$ edge can be conveniently used for the investigation of Ce compounds [16]. We have shown that different parts of the spectrum, corresponding to final states with different $4f$ occupancy, are separately enhanced, and that the details of the resonance are directly related to the strength of configuration mixing in the ground state. In the present paper we investigate the spectral changes and the variations of the relative intensities of the $4f$ and conduction band signals across the resonance. $CeRh_3$, a metallic compound where the $4f$-band hybridization is very strong, is an interesting test case, because the emission from $4f$ states largely dominates the band contribution in the conventional IPES spectrum.

The resonant IPES (RIPES) measurements have been carried out in a dedicated ultra-high vacuum apparatus, which will be described elsewhere [17]. The polychromatic soft X-ray photons produced by the impact of a focalised monochromatic electron beam ($\Delta E \sim 0.3$ eV) are dispersed by a Bragg reflection from a cylindrical beryl (1010) crystal onto a position-sensitive detector, where the whole spectrum is accumulated. The useful interval of electron kinetic energies (875 eV $< E_k <$ 900 eV) is defined by the photon energy range accepted by the spectrograph, and the overall energy resolution (electrons plus photons) is ~ 0.7 eV. The polycrystalline $CeRh_3$ sample was prepared by melting high-purity constituents in an induction-melting furnace under argon atmoshpere, and later annealed and characterized by standard metallographic methods and X-ray diffraction. Clean surfaces were periodically prepared *in situ* by scraping with a diamond file. The sample temperature was 50 K in order to minimise outdiffusion of bulk impurities, especially oxygen.

The IPES spectra of metallic Ce compounds exhibit two characteristic cerium-derived features: a sharp, resolution-limited peak just above $E_F$, and a wider structure 4–5 eV above it [3]. The intensity ratio of the two structures varies substantially in different materials, and is correlated with the satellites intensity in the Ce core spectra. Within the framework of the Anderson model, the shallow peak represents the unresolved superposition of the Kondo or Abrikosov-Suhl resonance with its spin-orbit replica, and corresponds to final states with essentially $f^1$ character. The position and width of the Kondo resonance at $T = 0$ define the fundamental energy $\delta = k_B T_K$. Its intensity scales with $T/T_K$, and it is therefore a rapidly varying function of the hybridization between the $4f$ and the conduction band electrons. The presence of the unresolved spin-orbit ($4f_{7/2}$) replica, located ~ 300 meV above the Kondo resonance, produces a shift of the experimentally observed peak away from $E_F$. The second feature is the electron affinity peak, and corresponds to final states with mainly $f^2$ character.

On the basis of lattice parameter [18] and resistivity [19] measurements, $CeRh_3$ has been described as a typical «tetravalent» ($f^0$) Ce compound. It is however more appropriate to consider it as representative of the strong hybridization limit of the Anderson Hamiltonian, as also confirmed by photoemission and X-ray absorption data on the Ce $3d$ core levels [20]. Recently it was proposed that the $4f$ electrons in $CeRh_3$ could be treated within a band picture [21], but it was later shown that although state-of-the-art band structure calculations correctly reproduce the conduction band features, they fail to describe the $4f$ spectral function [22]. The conventional IPES spectrum of $CeRh_3$ is largely dominated by a strong $f^1$

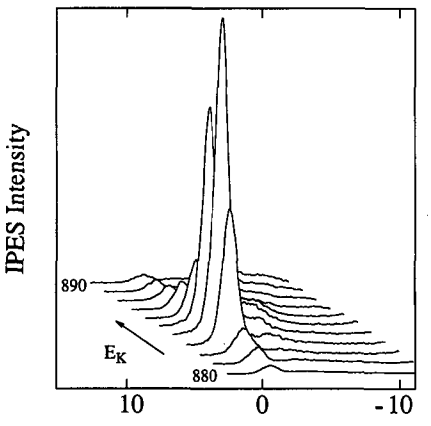


Fig. 1.

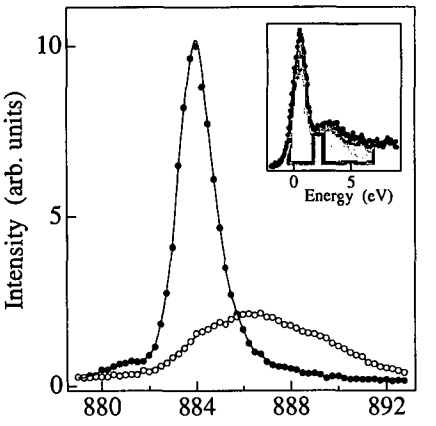


Fig. 2.

Fig. 1. – RIPES spectra of $CeRh_3$ measured near the Ce $M_5$ absorption edge. The spectra have been collected at electron kinetic energies variable between 880 eV and 890 eV in 1 eV steps, and the photon energy zero coincides with the position of the Fermi level at 880 eV.

Fig. 2. – Constant final state (CFS) curves obtained by integrating the IPES spectra within two energy windows (respectively, 2.5 and 5 eV wide) centered around the $f^1$ (●) and $f^2$ (○) structures. The integration windows are the shaded regions shown in the inset superposed to a spectrum measured at 880 eV.

peak 1 eV above $E_F$, while the $f^2$ structure can barely be observed [21, 22]. Both the position and the intensity of the $f^1$ peak indicate an unusually strong hybridization in this compound. The RIPES spectra of $CeRh_3$ collected across the Ce $M_5$ edge are shown in fig. 1. We observe that the overall spectral intensity is dramatically enhanced around $E_k$ = 884 eV, and rapidly drops both at lower and higher excitation energies. The intensity enhancement at 884 eV is of two orders of magnitude compared to the pre-edge spectrum. As discussed elsewhere [16], the resonance is the consequence of the quantum interference between a *direct* $4f$ IPES process, $4f^n + e^- \rightarrow 4f^{n+1} + h\nu$, and an *indirect* process involving the creation of a $3d$ core hole, $4f^n + e^- \rightarrow \underline{3d}\, 4f^{n+2} \rightarrow 4f^{n+1} + h\nu$, the two channels connecting the same initial and final states. In cerium-based materials, the resonance process is complicated by configuration mixing. Neglecting double occupancy ($U_{ff} = \infty$ limit) two configurations, $f^0$ and $f^1$, are present in the ground state, and the possible direct IPES transitions can schematically be described as: $4f^0 + e^- \rightarrow 4f^1 + h\nu_1$, and $4f^1 + e^- \rightarrow 4f^2 + h\nu_2$. The corresponding interfering channels are $4f^0 + e^- \rightarrow \underline{3d}\, 4f^2 \rightarrow 4f^1 + h\nu_1$ and, respectively, $4f^1 + e^- \rightarrow \underline{3d}\, 4f^3 \rightarrow 4f^2 + h\nu_2$. Two distinct resonances separated by $\sim 2$ eV are then observed [16], and different parts of the IPES spectum are amplified at different electron kinetic energies. The ratio $R$ between the peak values of the $f^1$ and $f^2$ spectral features is highly material dependent: it reflects the hybridization strength and the degree of configuration mixing in the ground state. $R$ is small in compounds like CeSb or $CeGe_2$, where hybridization between the $4f$ electrons and the conduction band is weak, but it rapidly increases with hybridization. The growth of the $f^1$ resonance correlates with the rapid transfer of spectral weight from the affinity peak to the Kondo peak in the IPES spectra [4]. $R$ is of the order of 1 in moderatly hybridized materials like $CePd_3$ or $CeNi_2$, and it can be much larger than 1 in extremely high $T_K$ compounds [16]. Tanaka and Jo have recently calculated the resonant IPES spectra of $CeNi_2$ within the AIM, taking into account the full multiplet structure, and have obtained a remarkable agreement with the experimental results [23].

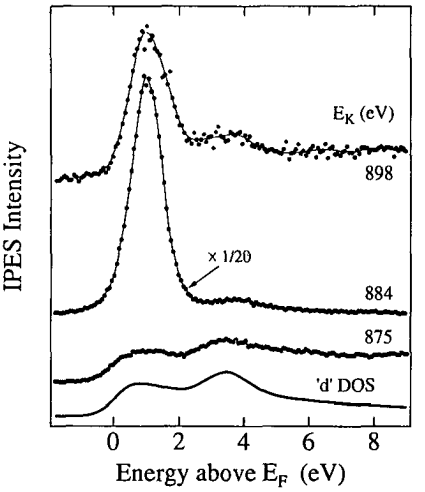


Fig. 3. – IPES spectra of $CeRh_3$ measured below (875 eV), at (884 eV) and above (898 eV) the $f^1$ resonance. The Fermi level is the energy zero for all spectra, and the intensity has been normalized to the acquisition time. Notice that the 884 eV spectrum has been scaleddown by a factor of 20. The solid line is a calculated partial density of states of $d$ symmetry, from ref. [21].

The RIPES spectra of fig. 1, as well as the energy dependence of the integrated $f^1$ and $f^2$ intensities shown in fig. 2, show that the $f^1$ signal is, as expected for such a strongly hybridized material, predominantly enhanced at the Ce $M_5$ edge ($R \gg 1$). Spectacular spectral changes however occur over a slightly wider excitation energy range. Fig. 3 shows the on-resonance spectrum ($E_k = 884$ eV), and two spectra measured well above ($E_k = 898$ eV) and below ($E_k = 875$ eV) the resonance. Besides an obvious overall intensity drop off-resonance, the lineshapes of the three spectra are dramatically different. The 898 eV spectrum is quite similar to the conventional IPES spectrum of $CeRh_3$, and the distinct shoulder at 3–4 eV which is the superposition of a signal from conduction band states of mainly $d$ symmetry, and of a weak $f^2$ contribution. An almost pure Ce $4f$ spectral function, on the other hand, is observed when the excitation energy is changed to 884 eV. The intensity gain is so large that at this energy an acceptable spectrum can be accumulated in only a few minutes, in contrast to the several hours required by a conventional IPES measurement. This represents a crucial improvement when reactive samples are studied. An even more striking spectral change, however, occurs between 884 and 875 eV. Here the $4f$ signal has essentially vanished, and a resolution-limited Fermi edge has appeared. The 875 eV spectrum is similar to IPES spectra of $CeRh_3$ measured at 10.5 eV, where the $4f$ cross-section is extremely small [15]. Moreover, a very good agreement is observed between the measured spectrum and the calculated partial density of states of $d$ symmetry of ref. [21]. A complete transition from an $f$-sensitive to a $d$-sensitive spectrum has therefore occurred between 884 eV and 875 eV. These results, and similar results we have obtained on various other Ce compounds, suggest that the $4f$ cross-section must present a minimum before the resonance. They confirm and extend an analogous observation on metallic cerium [13]. We cannot at this time assess the depth and width of the dip. However the very occurrence of an antiresonance is remarkable because, unlike the much studied $4d \rightarrow 4f$ giant resonance, the $3d \rightarrow 4f$ resonance is not expected to exhibit a simple Fano lineshape. Hundreds of multiplet lines in the intermediate states may in fact contribute to a complex resonance profile, as illustrated by the $3d$ X-ray absorption spectra of $Ce^{3+}$ ($f^1 \rightarrow \underline{3d}f^2$) and $Pr^{3+}$ ($f^2 \rightarrow \underline{3d}f^3$) [24].

Full multiplet calculations within the Anderson impurity model, like those performed in ref. [23] should clarify this intriguing point, and should also allow a quantitative analysis of the energy-dependent $4f$ spectrum.

In conclusion, we have shown that the character of the IPES spectrum of $CeRh_3$ changes from $4f$-sensitive at resonance, to conduction-band–sensitive a few eVs below resonance. The rapid cross-section variations offer the unique opportunity of varying the sensitivity to the $4f$ states by more than two orders of magnitude over a very small excitation energy range. We have exploited this possibility to identify and clearly separate for the first time the spectral contribution of the localized and the extended states in the arduous case of $CeRh_3$. The present results demonstrate the advantages offered by the intensity enhancement and the selectivity to the atomic symmetry and configuration of RIPES. RIPES appears as a powerful probe of the unoccupied states not only of Ce compounds, but more generally of correlated electron systems. We expect it to be well suited, for instance, for an analysis of the electronic configuration of Cu atoms in the superconducting cuprates, a possibility that is currently investigated in our laboratory.

* * *

We thank Profs. G. KAINDL and C. LAUBSCHAT for useful discussions and for bringing to our attention the work of the St. Petersburg group. This work has been supported by the Fonds National Suisse de la Recherche Scientifique.

## REFERENCES

[1] For a general review see: CONNERADE J. P., ESTEVA J.-M. and KARNATAK R. C. (Editors), *Giant Resonances in Atoms, Molecules and Solids* (Plenum, New York, N.Y.) 1987.
[2] DAVIS L. C., *J. Appl. Phys.*, 59 (1986) R25 and references therein.
[3] ALLEN J. W., OH S.-J., GUNNARSSON O., SCHÖNHAMMER K., MAPLE M. B., TORIKACHVILI M. S. and LINDAU I., *Adv. Phys.*, 35 (1986) 275.
[4] GUNNARSSON O. and SCHÖNHAMMER K., *Phys. Rev. B*, 28 (1983) 4315.
[5] BICKERS N. E., COX D. L. and WILKINS J. W., *Phys. Rev. B*, 36 (1987) 2036.
[6] PATTHEY F., IMER J.-M., SCHNEIDER W.-D., BECK H., BAER Y. and DELLEY B., *Phys. Rev. B*, 42 (1990) 8864.
[7] MALTERRE D., GRIONI M., WEIBEL P., DARDEL B. and BAER Y., *Phys. Rev. Lett.*, 68 (1992) 2656; *Phys. Rev. B*, 48 (1993) 10599.
[8] TJENG L. H., OH S.-J., CHO E. J., LIN H. J., CHEN C. T., GWEON G. H., PARK J. H., ALLEN J. W., SUZUKI T., MAKIVICH M. S. and COX D. L., *Phys. Rev. Lett.*, 71 (1993) 1419.
[9] ALLEN J. W., OH S.-J., LINDAU I. and JOHANSSON L. I., *Phys. Rev. B*, 29 (1984) 5927.
[10] BECKER U., KERKHOFF H. G., LINDLE D. W., KOBRIN P. H., FERRET T. A., HEIMANN P. A., TRUESDALE C. M. and SHIRLEY D. A., *Phys. Rev. B*, 34 (1986) 2858.
[11] LAUBSCHAT C., WESCHKE E., KALKOWSKI G. and KAINDL G., *Phys. Scr.*, 41 (1990) 124.
[12] WESCHKE E., LAUBSCHAT C., SIMMONS T., DOMKE M., STREBEL O. and KAINDL G., *Phys. Rev. B*, 44 (1991) 8304.
[13] CHAMBERLAIN M. B., BURR A. F. and LIEFELD R. J., *Phys. Rev. A*, 9 (1974) 663; *J. Vac. Sci. Technol. A*, 1 (1983) 1169.
[14] RIEHLE F., *Jpn. J. Appl. Phys.*, 17 (1978) Suppl. 17-2, 314.
[15] FORMICHEV V. A. and SHULAKOV A. S., *Phys. Scr.*, 41 (1990) 99.
[16] WEIBEL P., GRIONI M., MALTERRE D., DARDEL B. and BAER Y., *Phys. Rev. Lett.*, 72 (1994) 1252.
[17] WEIBEL P. *et al.*, in preparation.
[18] HARRIS I. R., NORMAN M. and GARDNER W. E., *J. Less Common Met.*, 29 (1972) 299.
[19] CATTANEO E., *Z. Phys. B*, 64 (1986) 305.

[20] KRILL G., KAPPLER J.-P., MEYER A., ABADLI L. and RAVET M. F., *J. Phys. F*, **11** (1981) 1713.
[21] WESCHKE E., LAUBSCHAT C., ECKER R., HÖHR A., DOMKE M., KAINDL G., SEVERIN L. and JOHANSSON B., *Phys. Rev. Lett.*, **69** (1992) 1792.
[22] MALTERRE D., GRIONI M., BAER Y., BRAICHOVICH L., DUÒ L., VAVASSORI P. and OLCESE G. L., *Phys. Rev. Lett.*, **73** (1994) 2005.
[23] TANAKA A. and JO T., *Proceedings of the International Conference on Strongly Correlated Electron Systems, Amsterdam, 1994*, to be published in *Physica B*.
[24] THOLE B. T., VAN DER LAAN G., FUGGLE J. C., SAWATZKY G. A., KARNATAK R. C. and ESTEVA J.-M., *Phys. Rev. B*, **32** (1993) 5107.

# Listes des publications

1. D. Malterre, M. Grioni, P. Weibel, B. Dardel and Y. Baer, "Temperature dependence of the *4f* spectral function in the Kondo system $CeSi_2$: evidence of the Kondo resonance smearing", *Europhys. Lett.* 20 445 (1992).
2. P. Weibel, M. Grioni, D. Malterre, B. Dardel and Y. Baer, "Strong temperature dependence of the Kondo peak in $YbAgCu_4$", *Z. Phys. B - Condensed Matter.*, 91, 337 (1993).
3. D. Malterre, M. Grioni, P. Weibel, B. Dardel and Y. Baer, "Evidence of a Kondo Scale from the Temperature Dependence of Inverse Photoemission Spectra of $CePd_3$", *Phys. Rev. Lett.* 68, 2656 (1992).
4. D. Malterre, M. Grioni, P. Weibel, B. Dardel and Y. Baer, "Correlation between Kondo temperature and photoemission spectral function in the $CeSi_x$ ($1.6 \leq x \leq 2$) system", *Phys. Rev. B* 48, 10599 (1993).
5. P. Weibel, M. Grioni, C. Hêche and Y. Baer, "A soft X-ray spectrometer for resonant inverse photoemission", *to be published in Review of Scientific instruments* 66, July 1995.
6. P. Weibel, M. Grioni, D. Malterre, B. Dardel and Y. Baer, "Resonant Inverse Photoemission: A New Probe of Correlated Systems", *Phys. Rev. Lett.* 72, 1252 (1994).
7. P. Weibel, M. Grioni, D. Malterre, O. Manzardo, Y. Baer and G. Olcese, "Resonance and anti-resonance in inverse photoemission: discriminating localized and extended states in cerium systems", *Europhys. Lett.* 29, 629 (1995).

Le texte complet de la thèse se trouve à l'Institut de Physique de l'Université de Neuchâtel, Breguet 1, Neuchâtel.